Available at www.ComputerScienceWeb.com
POWERED BY SCIENCE DIRECT®

Robotics and Autonomous Systems 43 (2003) 257–282

Robotics and Autonomous Systems

www.elsevier.com/locate/robot

A distributed motion coordination strategy for multiple nonholonomic mobile robots in cooperative hunting operations

Hiroaki Yamaguchi

Research into Artifacts, Center for Engineering, The University of Tokyo, Komaba 4-6-1, Meguro-ku, Tokyo 153-8904, Japan

Communicated by F.C.A. Groen

Abstract

This paper presents a distributed smooth time-varying feedback control law for coordinating motions of multiple nonholonomic mobile robots of the Hilare-type to capture/enclose a target by making troop formations. This motion coordination is a cooperative behavior for security against invaders in surveillance areas. Each robot in this control law has its own coordinate system and it senses a target/invader, other robots and obstacles, to achieve this cooperative behavior without making any collision. Each robot especially has a two-dimensional control input referred to as a "formation vector" and the formation is controllable by the vectors. The validity of this control law is supported by computer simulations.

Keywords: Nonholonomic mobile robotic system; Mobile robot troop; Distributed control; Smooth time-varying feedback; Formation controllability; Cooperative behavior

1. Introduction

1.1. Objective of research

Nonholonomy is a central issue on controlling a mobile robot in a single operation or multiple mobile robots in a collective operation. There have been significant methodologies for asymptotically/exponentially stabilizing nonholonomic mechanical systems, including unicycle-type mobile robots, car-like mobile robots, and mobile robots towing trailers, in single operations by smooth or non-smooth time-varying feedback control laws [33,35] (see in detail [12]). These control laws are quite powerful on controlling such single nonholonomic mechanical systems. However, it is not straightforward to apply them to controlling multiple nonholonomic mechanical systems interacting with each other in collective operations. Our objective is to develop a quantitative theoretical scheme which guarantees asymptotic/exponential stability and formation controllability on coordinating the motions of the multiple nonholonomic mobile robots of the Hilare-type to make formations in a distributed fashion. Hilare [18] is a historical mobile robot built in 1977 at LAAS, France, and it is kinematically equivalent to a unicycle-type mobile robot. We present, in this paper, a distributed smooth time-varying feedback control law whose asymptotic stability is guaranteed in a mathematical framework, averaging theory [34], and in which formation controllability holds.

E-mail address: yamaguch@race.u-tokyo.ac.jp (H. Yamaguchi).

doi:10.1016/S0921-8890(03)00037-X

1.2. Motion coordination of multiple mobile robots

Coordinating behaviors of multiple mobile robots is crucial on making cooperation among them to achieve tasks that single mobile robots cannot manage such as lunar-base construction by bulldozer-type mobile robots [8], a toxic waste cleanup by mobile robots [30], panel construction by mobile robots equipped with manipulators [21,22], cooperative transportation/manipulation of a large object by mobile robots [2,15,19,24,25,27,50] and by two four-legged robots [1], and surveillance and exploration by mobile robots [9,17,29,36]. These tasks are performed by sophisticated control methodologies designed according to each specific application of the mobile robots. Especially, the mobile robots are required to coordinate their motions on performing the tasks cooperatively. There are two control schemes for coordinating the motions, a model-based control scheme and a behavior-based control scheme. In the model-based control scheme, kinematics or dynamics of each mobile robot and interaction between the robots are modeled mathematically. In addition, quantitative theoretical issues such as stability and controllability are discussed rigorously. On the other hand, in the behavior-based control scheme, reactions of each robot to stimuli coming from other robots or working environment are designed according to each task. As we have described, we focus on developing a model-based control scheme, i.e., a quantitative theoretical scheme for coordinating the motions of the multiple nonholonomic mobile robots of the Hilare-type to make formations in a distributed fashion.

As one of typical examples of cooperative behavior in which motion coordination is required, let us consider cooperative transportation of an object carried by multiple mobile robots here briefly. Each robot in this case needs to keep a certain relative position to others which is determined by the geometric arrangement of the supporting points underneath the object. In a centralized control methodology, there is a supervisor who specifies the goal configuration of the object and who also specifies a geometric path connecting the object current configuration and its goal configuration. This geometric path turns into a trajectory when it is associated with some timing law. Once the motion of the object is determined, the motion of each mobile robot is also uniquely determined, satisfying the constraint that is the geometric arrangement of the supporting points. Of course, when each robot has nonholonomic constraints, the supervisor cannot specify an arbitrary path (or trajectory). The nonholonomic constraints physically mean that the robot wheels roll without slipping and such constraints reduce the instantaneous mobility of the robot, while it is still controllable in its configuration space. In a distributed control methodology, there is no such supervisor and each robot is allowed to communicate only with its neighboring robots on determining its motion in many cases. If there is an appropriate distributed motion coordination strategy, then the mobile robots cooperatively achieve transporting the object to the goal configuration. It is more difficult to make the object follow a desired path (or trajectory) exactly without the supervisor.

1.3. Mission of multiple nonholonomic mobile robots in hunting behavior

We suppose, in this paper, that multiple nonholonomic mobile robots of the Hilare-type capture/enclose a target/invader by making troop formations in surveillance areas. A distributed control law [43,47] to perform such cooperative behavior has been presented in the case of multiple holonomic mobile robots. However, it is more difficult to perform this behavior by multiple nonholonomic mobile robots of the Hilare-type in a distributed fashion, which we describe in this paper. In a centralized control methodology to perform this task, a supervisor specifies the goal positions of all the robots around the target and it also specifies the paths (or trajectories) connecting the current and goal positions of them. The supervisor specifically plans the motion of each robot, avoiding collisions with the other robots and obstacles, in order to make group formations capturing/enclosing the target. One of the drawbacks of the centralized control methodology is that the computation and communication burdens imposed on the supervisor planning the motions of all the robots and sending commands to each of them significantly increase when the number of the robots gets larger. In the worst case, the centralized control methodology loses simultaneity and its motion planning finally becomes off-line. In an off-line motion planning, the supervisor is supposed to have the information describing the geometrical arrangement of static obstacles, e.g., walls, tables, desks, chairs, and sofas, in the working environment. The supervisor is also supposed to have the information describing the movements of mobile obstacles. When we put some static or mobile obstacles that are unknown to the supervisor, it is required to plan the motions of all the robots over again. This means that the centralized control methodology is lacking adaptability to the variation of the working environment. In a distributed control methodology, there is no such supervisor and each robot determines its motion referring to its relative position to other robots and the target, in order to achieve this task. Especially, if there is an appropriate distributed motion coordination strategy, then we do not need to resort to having a powerful planner who monitors the positions of all the robots and who plans their motions and who also sends commands to each of them. In other words, the distributed control methodology enables the robots to perform this task, belonging to the category of an on-line motion planning. Of course, in both the centralized and distributed control methodologies, it is a challenging problem to overcome nonholonomic constraints on coordinating the motions of multiple nonholonomic mobile robots.

To capture/enclose a target by making troop formations in a distributed control methodology, each mobile robot (which is a nonholonomic mobile robot of the Hilare-type) in a troop needs to control its relative position to other robots, which means that each robot has relative position feedback. Via this feedback, the robots interact with each other. It follows from this that the robots making formations compose a large-scale visually articulated multi-body system, and we need to consider the stability and controllability issues of the whole system on performing this task. It is certainly a challenging problem to asymptotically stabilize mechanical systems with nonholonomy to their desired configurations. This is because, as Brockett's theorem [7] suggests, controllable systems without drift, including unicycle-type mobile robots (which are kinematically equivalent to nonholonomic mobile robots of the Hilare-type), car-like mobile robots, mobile robots towing trailers, cannot be asymptotically stabilized by smooth time-invariant feedback control laws. For the purpose of performing the task, we need to develop a novel distributed control law (which is required to be not a smooth time-invariant feedback control law) to asymptotically stabilize a troop consisting of multiple nonholonomic mobile robots of the Hilare-type which is regarded as a large-scale visually articulated multi-body system. Let us summarize the previously presented significant methodologies for asymptotically/exponentially stabilizing nonholonomic mobile robots to their desired configurations via smooth time-varying, discontinuous and non-smooth time-varying feedback control laws, below.

1.4. Feedback control for nonholonomic mobile robots

Samson [32] has initiated to examine smooth time-varying feedback control laws and he has presented a feedback control law for a unicycle-type mobile robot. Motivated by potentiality of such feedback control laws, Coron [11] has proven that smooth time-varying feedback control laws can asymptotically stabilize controllable systems without drift. This exploit has shown the existence of the control laws, and then Pomet [31] has presented an explicit design procedure for the systems based on the Lyapunov second method. Teel et al. [39] have presented another smooth time-varying feedback control law to asymptotically stabilize mechanical systems in "power form" which is derived from "chained form". This chained form is widely used on kinematically describing a large class of controllable systems without drift, including unicycle-type mobile robots, car-like mobile robots and mobile robots towing trailers, although this class does not comprehend all controllable systems without drift. Samson [33] has presented "skew-symmetric chained form" that is also derived from chained form, and he has shown that mechanical systems in this form can be also asymptotically stabilized by a smooth time-varying feedback control law (see [12] in detail). This skew-symmetric chained form is suited for a Lyapunov-like stability analysis. These time-varying feedback control laws can guarantee asymptotic stability but cannot guarantee exponential stability. A slow convergence rate is actually a drawback of these control laws. To overcome this drawback, M'Closkey and Murray [28] have established a methodology to convert any asymptotic stabilizer for controllable systems without drift into an exponential stabilizer using time-varying homogeneous feedback, and they have shown that the convergence rates of the asymptotic stabilizers by Pomet [31] and by Teel et al. [39] are significantly improved by their methodology.

As alternatives, discontinuous and non-smooth feedback control laws have been explored. Bloch et al. [5] have presented a discontinuous analytic feedback control law to asymptotically stabilize a class of nonholonomic mechanical systems. Unlike other control laws, the dynamics as well as the kinematics of the systems are considered and both velocity and torque inputs are allowed to be used in this control law. Canudas de Wit and Sørdalen [10] have presented a discontinuous feedback control law to exponentially stabilize a unicycle-type mobile robot in three-dimensional chained form. Sørdalen and Egeland [35] have extended the control law and they have presented a non-smooth time-varying feedback control law to exponentially stabilize all mechanical systems in chained form (see [12] in detail).

The feedback control laws mentioned above are supposed to control a single nonholonomic mechanical system and there have been no distributed control law to asymptotically stabilize multiple nonholonomic mechanical systems interacting with each other. Therefore, although a nonholonomic mobile robot of the Hilare-type is kinematically the simplest mobile robot, it is certainly challenging to establish a distributed feedback control law for asymptotically stabilizing multiple nonholonomic mobile robots of the Hilare-type to capture/enclose the target by making troop formations.

1.5. Formation control for multiple mobile robots

Sugihara and Suzuki [37,38] have first examined a distributed motion coordination strategy to make group formations of multiple holonomic mobile robots that are free to move on a plane, i.e., that can move in any direction instantaneously. They have specifically presented an algorithm that enables the robots to make circle formations. Although the final formation is not predicted quantitatively, they have derived such algorithm heuristically and they have confirmed its validity in computer simulations. The multiple mobile robots in this motion coordination strategy are homogeneous, which means that there is no stratification, i.e., there is no leader-robot and no follower-robot and no mediator-robot between them. However, we often use such stratification in motion planning of the multiple mobile robots. For instance, in a case where many mobile robots operate to pass a corridor, a robot follows another in front of itself as a follower. The robot followed is a leader. Following some robots in front makes an efficient flow of the robots. There have also been presented significant methodologies to make formations of the multiple mobile robots using the leader–follower stratification. Balch et al. [3,4] have first showed behavior-based formation control for making four formations, line, column, diamond and wedge, using a leader–follower approach. Each robotic vehicle is nonholonomic and it has some reactions designed for making these formations. This collective behavior has been successfully demonstrated by excellent experiments. Desai et al. [13,14] and Fierro et al. [16] have presented feedback control laws for navigating multiple nonholonomic mobile robots in a leader–follower operation so as to make formations. The leader-robot is required to keep moving on a pre-planned path, and each of the remaining robots is a follower-robot following the leader-robot or the other robot moving in front of itself. Although all the robots have nonholonomic constraints on their mobility, moving the robots enables them to control their relative positions between them. Since the robots in this case keep moving/marching until they make desired formations, it is not straightforward to apply their control laws to our task in which the robots capture/enclose the target/invader by making troop formations. Also, in our task, we do not need to have a supervisor who specifies which robot is a leader and which robot is a follower. We focus on making formations of the multiple mobile robots which are homogeneous.

Motivated by Sugihara and Suzuki's work [37,38], Yamaguchi and Beni [40,41,48] have started to explore mathematical formulas for making formations of the holonomic mobile robots, and they have shown that there exists a distributed control scheme which guarantees stability of the robots and controllability of the formation. Yamaguchi [42,43,47,49] has modified this control scheme and he has derived a methodology that enables the holonomic mobile robots to prevent invasions by making formations adapting to geometrical constraints of their working environment [42,49], and he has also derived a methodology that enables the holonomic mobile robots to capture/enclose a target/invader by making troop formations [43,47]. These methods [37,38,40–43,47–49] commonly have a presupposition that all the robots are free to move on a plane, i.e., they are holonomic mobile robots. Breaking such presupposition, Yamaguchi and Burdick [44,46] have shown the existence of a distributed smooth time-varying feedback control law that enables multiple nonholonomic mobile robots of the Hilare-type to make formations. Especially, the control law guarantees stability of the robots and controllability of the formation as the holonomic cases of [40,41]. Yamaguchi [45] has modified the distributed smooth time-varying feedback control law and he has shown that it is also possible to make the nonholonomic mobile robots of the Hilare-type capture/enclose a target/invader by making troop formations the same as the holonomic cases of [43,47], which we describe in this paper.

1.6. Summary of paper

Unlike other control laws which are supposed to asymptotically/exponentially stabilize a single nonholonomic mechanical system and which has particular form on kinematically describing the system, the distributed smooth time-varying feedback control law presented in this paper asymptotically stabilizes multiple nonholonomic mobile robots of the Hilare-type interacting with each other and the control law does not use any particular form. Asymptotic stability of the control law is guaranteed in a mathematical framework, averaging theory [34]. To prove its asymptotic stability we apply a theorem in averaging theory given by Eckhaus/Sanchez-Palencia (see [34, p. 70]). We specifically deal with a matrix whose components are averaged over time by integration and whose eigenvalue distribution explicitly describes stability of this control law. Since the components of this matrix are integral functions, its eigenvalue distribution is analytically shown by Hölder's inequality (see [51, p. 33]), in functional analysis. Therefore, stability analysis of this control law is given in averaging theory and it is technically related with functional analysis.

This paper is organized as follows. In Section 2, we give the models of each robot and a robot troop that pursues and tries to capture/enclose a target/invader in surveillance areas. In Section 3, we propose a distributed smooth time-varying feedback control law and we show its asymptotic stability. In Section 4, we describe formation controllability of this control law. In Section 5, we give computer simulations supporting the validity of this control law. Finally, in Section 6, we give conclusions.

2. Hunting behavior by mobile robot troops

We consider (n) mobile robots, a target and (m) obstacles on a plane. Each mobile robot is a nonholonomic mobile robot of the Hilare-type that has two wheels driven independently. We label each robot R_i and we also label each obstacle O_j. However, these labels are not intrinsic to this method. Each robot does not need to know its own label, other robots' and obstacles' labels. We denote with TARGET the target, and we also denote with Σ_i the coordinate system of R_i. Each robot senses its relative position to other robots, TARGET and obstacles in its own coordinate system, Σ_i. To express the positions of all the robots in a common coordinate system, we define a static coordinate system, Σ_0. To express the velocity of R_i, we also define another coordinate system, Σ_i^0, whose origin is common to that of Σ_0 and whose orientation is common to that of Σ_i (see Fig. 1). These coordinate systems, Σ_0 and Σ_i^0, are unknown to R_i. Each R_i knows only its own coordinate system, Σ_i.

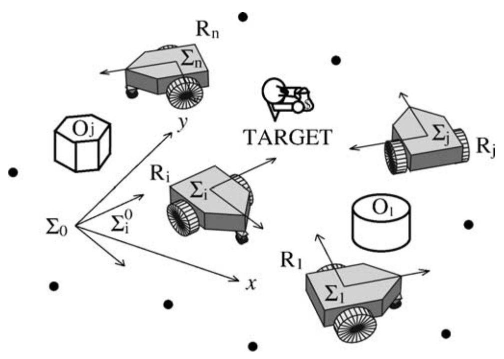

Fig. 1. Mobile robots, obstacles and TARGET on a plane.

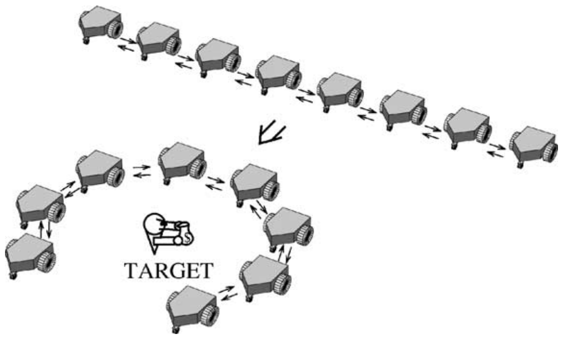

Fig. 2. A mobile robot troop.

Let us consider the (n) mobile robots in an open chain configuration that is referred to as a "strongly connected graph" in graph-theory. We suppose that this configuration is always static (see Fig. 2). A robot at the start of an arrow tries to keep a certain relative position to another at the end of the arrow, to make formations with other robots. We call these robots as a mobile robot troop, when they move toward TARGET in order to capture/enclose it by making troop formations. Although the control strategy presented in this paper is independent of the configuration of the troop, we consider only the cases of an "open chain troop" (see Fig. 2), because the mission of this troop is to capture/enclose TARGET by making an arc-like formation. Of course, in this operation, each robot avoids collisions with other robots, obstacles and TARGET.

3. Robot control

3.1. Desired velocity

Since, as we have described, the (n) mobile robots form a strongly connected configuration, at least one arrow goes from a robot to another. The (n) robots are especially in an open chain configuration. To perform this cooperative hunting operation, we define an attraction which binds the robots sensing each other, and we regard the (n) robots bound in this open chain configuration as a string. We define another attraction between each robot and TARGET. This attraction works only when the robot senses TARGET, and it drives this string to approach TARGET for capturing/enclosing it. We also define a two-dimensional vector given to each robot. This vector physically means that the robot is pulled in the direction of the vector and its pulling strength is proportional to the norm of the vector. The vector is referred to as a "formation vector" and it is used for controlling the shape of the string around TARGET. In other words, this vector is a control input for capturing/enclosing TARGET by the formation of the robots. In the following, we describe this control strategy more mathematically. We denote with L_i the set of robots to which arrows go from R_i. To make formations, R_i tries to keep a certain relative position to the robots in L_i. It also tries to keep a certain relative position to TARGET, to enclose it by making troop formations with other robots. Let us assume that at least one mobile robot in the troop can see TARGET. The robot, R_i, also controls its relative position to other robots, obstacles and TARGET, to avoid collisions with them. We denote with M_i the set of robots and we also denote with N_i the set of obstacles, when they are sensed by R_i for collision avoidance. The set, M_i, does not include $\mathrm{R}_j \in \mathrm{L}_i$. In this feedback control law, R_i tries to move at its desired velocity that is affected linearly by its relative position to the robots in L_i and to TARGET, in order to enclose it by making troop formations with other robots. The desired velocity of R_i is also affected linearly by its relative position to the robots in M_i, the obstacles in N_i and TARGET, to avoid collisions with them. Moreover, the desired velocity is affected linearly by a vector, ${}^t(d^i_{xi}, d^i_{yi})$, referred to as a "formation vector". The upper suffix, "i" means that the vector is expressed in the coordinate system of R_i, i.e., in Σ_i. Of course, any vector without this upper suffix is expressed in the static coordinate system, Σ_0. This notation rule is applied to the expression of any vector below. Formally, we express the desired velocity of R_i as:

$$\tilde{\boldsymbol{v}}^i_i = \begin{pmatrix} \tilde{v}^i_{xi} \\ \tilde{v}^i_{yi} \end{pmatrix} = \sum_{j\in L_i} \tau_{ij} \begin{pmatrix} x^i_j \\ y^i_j \end{pmatrix} + \tau_i \begin{pmatrix} x^i_t \\ y^i_t \end{pmatrix} + \begin{pmatrix} d^i_{xi} \\ d^i_{yi} \end{pmatrix} + \sum_{j\in \mathrm{OBJECTS}} \delta_{ij} \left\{ \begin{pmatrix} x^i_j \\ y^i_j \end{pmatrix} - D \begin{pmatrix} x^i_j \\ y^i_j \end{pmatrix} \bigg/ \left| \begin{pmatrix} x^i_j \\ y^i_j \end{pmatrix} \right| \right\}, \quad (1)$$

$$\delta_{ij} = \begin{cases} \delta & |{}^t(x^i_j, y^i_j)| \le D, \\ 0 & |{}^t(x^i_j, y^i_j)| > D, \end{cases} \qquad j \in \mathrm{OBJECTS} = L_i \cup M_i \cup N_i \cup \mathrm{TARGET},$$

where $\tilde{\boldsymbol{v}}^i_i$ is the desired velocity of R_i in Σ_i; ${}^t(x^i_j, y^i_j)$, $j \in L_i \cup M_i$, is the position of $R_j \in L_i \cup M_i$ in Σ_i, i.e., the relative position of $R_j \in L_i \cup M_i$ to R_i in Σ_i; ${}^t(x^i_j, y^i_j)$, $j \in N_i$, is the position of a point on the surface of $O_j \in N_i$ in Σ_i and the point is sensed by R_i for collision avoidance, i.e., the relative position of the sensed point to R_i in Σ_i; ${}^t(x^i_t, y^i_t) = {}^t(x^i_j, y^i_j)$, $j \in$ TARGET, is the position of TARGET in Σ_i, i.e., the relative position of TARGET to R_i in Σ_i; ${}^t(d^i_{xi}, d^i_{yi})$ is the formation vector of R_i; $\tau_{ij} > 0$, $j \in L_i$, is the attraction coefficient of R_i to $R_j \in L_i$; τ_i is the attraction coefficient of R_i to TARGET, and $\tau_i = \tau > 0$ when R_i can see TARGET, and $\tau_i = 0$ when R_i cannot see TARGET. Physically, $\tau_{ij}\,{}^t(x^i_j, y^i_j)$ in the first term of Eq. (1) means that R_i is attracted to R_j. The second term means that R_i is attracted to TARGET. The third term means that R_i is pulled in the direction of ${}^t(d^i_{xi}, d^i_{yi})$. The fourth term means that R_i is repulsed from $R_j \in L_i \cup M_i$, the surface of $O_j \in N_i$ and TARGET as an artificial potential field [6,20,26] exists. This repulsion works only in cases where at least one of the relative distances of R_i to them is shorter than D. The coefficient, δ_{ij}, $j \in L_i \cup M_i$, is the repulsion coefficient of R_i from $R_j \in L_i \cup M_i$; δ_{ij}, $j \in N_i$, is the repulsion coefficient of R_i from the surface of $O_j \in N_i$, and $\delta_{it} = \delta_{ij}$, $j \in$ TARGET, is the repulsion coefficient of R_i from TARGET. The scalar, δ, is positive.

The desired velocity, $\tilde{\boldsymbol{v}}^i_i$, is expressed in the static coordinate system, Σ_0, as:

$$\begin{aligned}\tilde{\boldsymbol{v}}_i &= \begin{pmatrix} \tilde{v}_{xi} \\ \tilde{v}_{yi} \end{pmatrix} = \rho_i \begin{pmatrix} \tilde{v}^i_{xi} \\ \tilde{v}^i_{yi} \end{pmatrix} \\ &= \sum_{j\in L_i} \tau_{ij}\rho_i \begin{pmatrix} x^i_j \\ y^i_j \end{pmatrix} + \tau_i\rho_i \begin{pmatrix} x^i_t \\ y^i_t \end{pmatrix} + \rho_i \begin{pmatrix} d^i_{xi} \\ d^i_{yi} \end{pmatrix} + \sum_{j\in \mathrm{OBJECTS}} \delta_{ij}\rho_i \left\{ \begin{pmatrix} x^i_j \\ y^i_j \end{pmatrix} - D \begin{pmatrix} x^i_j \\ y^i_j \end{pmatrix} \bigg/ \left| \begin{pmatrix} x^i_j \\ y^i_j \end{pmatrix} \right| \right\} \\ &= \sum_{j\in L_i} \tau_{ij} \left\{ \begin{pmatrix} x_j \\ y_j \end{pmatrix} - \begin{pmatrix} x_i \\ y_i \end{pmatrix} \right\} + \tau_i \left\{ \begin{pmatrix} x_t \\ y_t \end{pmatrix} - \begin{pmatrix} x_i \\ y_i \end{pmatrix} \right\} + \begin{pmatrix} d_{xi} \\ d_{yi} \end{pmatrix} \\ &\quad + \sum_{j\in \mathrm{OBJECTS}} \delta_{ij} \left[\left\{ \begin{pmatrix} x_j \\ y_j \end{pmatrix} - \begin{pmatrix} x_i \\ y_i \end{pmatrix} \right\} - D \left\{ \begin{pmatrix} x_j \\ y_j \end{pmatrix} - \begin{pmatrix} x_i \\ y_i \end{pmatrix} \right\} \bigg/ \left| \begin{pmatrix} x_j \\ y_j \end{pmatrix} - \begin{pmatrix} x_i \\ y_i \end{pmatrix} \right| \right], \end{aligned} \quad (2)$$

$$\delta_{ij} = \begin{cases} \delta & |{}^t(x_j, y_j) - {}^t(x_i, y_i)| \le D, \\ 0 & |{}^t(x_j, y_j) - {}^t(x_i, y_i)| > D, \end{cases} \qquad j \in \mathrm{OBJECTS} = L_i \cup M_i \cup N_i \cup \mathrm{TARGET},$$

where ${}^t(\tilde{v}_{xi}, \tilde{v}_{yi})$ is the desired velocity of R_i in Σ_0; ρ_i is the transformation matrix from Σ^0_i to Σ_0; ${}^t(x_j, y_j)$, $j \in L_i \cup M_i$, is the position of $R_j \in L_i \cup M_i$ in Σ_0; ${}^t(x_j, y_j)$, $j \in N_i$, is the position of a point on the surface of

O_j, $j \in N_i$, in Σ_0 and the point is sensed by R_i for collision avoidance; ${}^t(x_t, y_t) = {}^t(x_j, y_j)$, $j \in$ TARGET, is the position of TARGET in Σ_0, and ${}^t(d_{xi}, d_{yi})$ is ${}^t(d^i_{xi}, d^i_{yi})$ transformed by ρ_i and it is expressed in Σ_0.

3.2. Desired system

Let us consider a case where each robot is holonomic and it can move at its desired velocity, i.e., Eq. (3) holds

$$\begin{pmatrix} \dot{x}_i \\ \dot{y}_i \end{pmatrix} = \begin{pmatrix} \tilde{v}_{xi} \\ \tilde{v}_{yi} \end{pmatrix}. \tag{3}$$

Although, in fact, each robot is a nonholonomic mobile robot of the Hilare-type and it cannot move sideways, we dare to assume this case here and let us discuss stability of the robot controlled by Eq. (3) in this subsection. We refer to such robotic system as a "desired system". Since the robot in this control law tries to move at its desired velocity, at least this desired system should be asymptotically stable. To analyze stability of the desired system, we rewrite Eq. (3) as:

$$\begin{pmatrix} \dot{\boldsymbol{x}} \\ \dot{\boldsymbol{y}} \end{pmatrix} = \begin{pmatrix} B+C-\Delta-\Lambda & 0 \\ 0 & B+C-\Delta-\Lambda \end{pmatrix} \begin{pmatrix} \boldsymbol{x} \\ \boldsymbol{y} \end{pmatrix} + \begin{pmatrix} \Delta & 0 \\ 0 & \Delta \end{pmatrix} \begin{pmatrix} x_t \boldsymbol{v}_1 \\ y_t \boldsymbol{v}_1 \end{pmatrix} + \begin{pmatrix} \boldsymbol{d_x} \\ \boldsymbol{d_y} \end{pmatrix} + \begin{pmatrix} \boldsymbol{\xi_x} \\ \boldsymbol{\xi_y} \end{pmatrix}, \tag{4}$$

$$\boldsymbol{x} = {}^t(x_1, x_2, \dots, x_n), \quad \boldsymbol{y} = {}^t(y_1, y_2, \dots, y_n), \quad \boldsymbol{d_x} = {}^t(d_{x1}, d_{x2}, \dots, d_{xn}), \quad \boldsymbol{d_y} = {}^t(d_{y1}, d_{y2}, \dots, d_{yn}),$$

$$\boldsymbol{v}_1 = {}^t(1, 1, \dots, 1), \qquad \Delta = \mathrm{diag}(\tau_1, \tau_2, \dots, \tau_n), \quad \Lambda = \mathrm{diag}\left(\sum_{j \in \mathrm{N}_1 \cup \mathrm{TARGET}} \delta_{1j}, \dots, \sum_{j \in \mathrm{N}_n \cup \mathrm{TARGET}} \delta_{nj} \right),$$

$$\boldsymbol{\xi_x} = {}^t(\xi_{x1}, \xi_{x2}, \dots, \xi_{xn}), \qquad \boldsymbol{\xi_y} = {}^t(\xi_{y1}, \xi_{y2}, \dots, \xi_{yn}),$$

$$\xi_{xi} = \sum_{j \in \mathrm{N}_i \cup \mathrm{TARGET}} \delta_{ij} x_j - \sum_{j \in \mathrm{OBJECTS}} \frac{\delta_{ij} D (x_j - x_i)}{|{}^t(x_j, y_j) - {}^t(x_i, y_i)|},$$

$$\xi_{yi} = \sum_{j \in \mathrm{N}_i \cup \mathrm{TARGET}} \delta_{ij} y_j - \sum_{j \in \mathrm{OBJECTS}} \frac{\delta_{ij} D (y_j - y_i)}{|{}^t(x_j, y_j) - {}^t(x_i, y_i)|}, \quad \mathrm{OBJECTS} = \mathrm{L}_i \cup \mathrm{M}_i \cup \mathrm{N}_i \cup \mathrm{TARGET},$$

where the matrix, $B \in \mathbf{R}^{n\times n}$, has components defined as: $b_{ij,i\neq j} = \tau_{ij\in \mathrm{L}_i} > 0$; $b_{ij,i\neq j} = \tau_{ij\notin \mathrm{L}_i} = 0$, and $b_{ii} = -\sum_{j=1, j\neq i}^{n} b_{ij}$. The matrix, $C \in \mathbf{R}^{n\times n}$, has components defined as: $c_{ij,i\neq j} = \delta_{ij\in \mathrm{L}_i\cup \mathrm{M}_i}$; $c_{ij,i\neq j} = \delta_{ij\notin \mathrm{L}_i\cup \mathrm{M}_i} = 0$, and $c_{ii} = -\sum_{j=1, j\neq i}^{n} c_{ij}$. The set, M_i, does not include $\mathrm{R}_j \in \mathrm{L}_i$. As we have described, the troop has a strongly connected configuration, so that $b_{ii} < 0$, $i = 1, 2, \dots, n$. Since the diagonal components of B are negative and the non-diagonal ones are not negative, B is a compartment matrix. The matrix, C, is also a compartment matrix. Then, it follows from $(B + C - \Delta - \Lambda)\boldsymbol{v}_1 \leq 0$ that $(B + C - \Delta - \Lambda)$ is asymptotically stable [23]. In Eq. (4), the norms of $\boldsymbol{\xi_x}$ and $\boldsymbol{\xi_y}$ are finite, because ${}^t(\xi_{xi}, \xi_{yi})$ is the summation of the two terms: one is the summation of $\delta_{ij}\,{}^t(x_j, y_j)$, $j \in \mathrm{N}_i \cup$ TARGET, and the other is the summation of the normalized vectors, and the norm of each vector is $\delta_{ij} D$ (see Eq. (4)). In addition, we design the norm of ${}^t(d_{xi}, d_{yi})$ to be finite. Then, $\boldsymbol{x}$ and $\boldsymbol{y}$ are stable and they are determined by the formation vectors, the positions of TARGET and the obstacles. Actually, the holonomic mobile robots which have the formation vectors determined as in Fig. 6 capture/enclose TARGET by making an arc-like formation (see [43,47]). In the following, we show that, even if each robot is a nonholonomic mobile robot of the Hilare-type, this robotic system is still asymptotically stable the same as the case where each robot is holonomic and the robots achieve this cooperative hunting behavior.

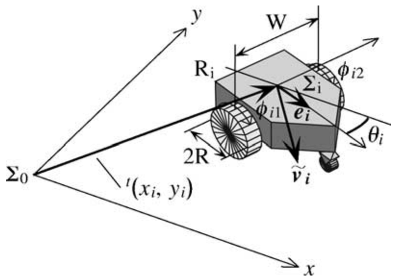

Fig. 3. A Hilare-type mobile robot.

3.3. Control inputs for robot wheels

A Hilare-type mobile robot has two wheels that are driven independently. Rotating these wheels, this mobile robot controls its position and orientation. In particular, it is possible for this type of robot to change its orientation without moving in any direction. We denote the position of R_i with ${}^t(x_i, y_i)$ and its orientation with θ_i in the static coordinate system, Σ_0. We also denote the rotation angles of its two wheels with ϕ_{i1} and ϕ_{i2}, respectively, and the radius of the wheel with R and the width between the wheels with W (see Fig. 3). Its moving velocity and its angular velocity of its orientation are given as:

$$\begin{pmatrix} \dot{x}_i \\ \dot{y}_i \\ \dot{\theta}_i \end{pmatrix} = \begin{pmatrix} \dfrac{R}{2}\cos\theta_i(\dot{\phi}_{i1}+\dot{\phi}_{i2}) \\ \dfrac{R}{2}\sin\theta_i(\dot{\phi}_{i1}+\dot{\phi}_{i2}) \\ \dfrac{R}{2W}(\dot{\phi}_{i1}-\dot{\phi}_{i2}) \end{pmatrix}. \tag{5}$$

We define $\boldsymbol{e}_i$ in Eq. (6) that is a unit vector and that is on an axis of Σ_i. The axis specifies the orientation of R_i, i.e., θ_i in the static coordinate system, Σ_0 (see Fig. 3). We also define $\boldsymbol{v}_i$ in Eq. (7) that is the velocity of R_i. These vectors, $\boldsymbol{e}_i$ and $\boldsymbol{v}_i$, are expressed in the static coordinate system, Σ_0.

$$\boldsymbol{e}_i = {}^t(\cos\theta_i, \sin\theta_i), \tag{6}$$

$$\boldsymbol{v}_i = {}^t(\dot{x}_i, \dot{y}_i) = \tfrac{1}{2}R(\dot{\phi}_{i1}+\dot{\phi}_{i2})\boldsymbol{e}_i. \tag{7}$$

As Eq. (7) shows, the robot can move only in the direction of the vector, $\boldsymbol{e}_i$, and it cannot move in its sideways direction. This means that the robot cannot move at the desired velocity, $\tilde{\boldsymbol{v}}_i$, as long as $\boldsymbol{e}_i$ is not parallel to $\tilde{\boldsymbol{v}}_i$. For that reason, we take a projection of $\tilde{\boldsymbol{v}}_i$ onto the axis of Σ_i specifying θ_i in Σ_0 and we determine the robot velocity, $\boldsymbol{v}_i$, in order for it to be the same as the projection, as:

$$\boldsymbol{e}_i \cdot \boldsymbol{v}_i = \boldsymbol{e}_i \cdot \tilde{\boldsymbol{v}}_i. \tag{8}$$

From Eqs. (7) and (8), the summation of the angular velocities of the two wheels is determined as:

$$\dot{\phi}_{i1}+\dot{\phi}_{i2} = \frac{2}{R}\boldsymbol{e}_i \cdot \tilde{\boldsymbol{v}}_i. \tag{9}$$

Since the vector, $\tilde{\boldsymbol{v}}_i$, linearly depends on the relative position of R_i to other robots, TARGET and obstacles, the right-hand side of Eq. (9) is state feedback. When the robot does not change its orientation, $\boldsymbol{e}_i$ is static and this feedback is smooth time-invariant feedback. On the other hand, when the robot changes its orientation dependently on time, this feedback is smooth time-varying feedback. Unless the robot changes its moving direction, the desired velocity, $\tilde{\boldsymbol{v}}_i$, can be perpendicular to $\boldsymbol{e}_i$. In the case where $\tilde{\boldsymbol{v}}_i \perp \boldsymbol{e}_i$, the projection of $\tilde{\boldsymbol{v}}_i$ onto the axis of Σ_i that specifies θ_i in Σ_0 is zero and the robot stops without capturing/enclosing TARGET by making troop formations with other robots. To avoid this case, we propose that each robot changes its orientation according to time. Specifically, we design the orientation to be a function of time as $\theta_i = \theta_i(t)$. This means that we use smooth time-varying feedback. Once this function is given and then the difference of the angular velocities between the wheels is determined as:

$$\dot{\phi}_{i1} - \dot{\phi}_{i2} = \frac{2W}{R}\dot{\theta}_i(t). \tag{10}$$

From Eqs. (9) and (10), the angular velocities of the wheels are uniquely determined as:

$$\dot{\phi}_{i1} = \frac{(\boldsymbol{e}_i \cdot \tilde{\boldsymbol{v}}_i + W\dot{\theta}_i(t))}{R}, \tag{11}$$

$$\dot{\phi}_{i2} = \frac{(\boldsymbol{e}_i \cdot \tilde{\boldsymbol{v}}_i - W\dot{\theta}_i(t))}{R}. \tag{12}$$

The inner product, $\boldsymbol{e}_i \cdot \tilde{\boldsymbol{v}}_i$, in Eqs. (11) and (12) can be rewritten as:

$$\boldsymbol{e}_i \cdot \tilde{\boldsymbol{v}}_i = \boldsymbol{e}_i^i \cdot \tilde{\boldsymbol{v}}_i^i, \tag{13}$$

where $\boldsymbol{e}_i^i$ and $\tilde{\boldsymbol{v}}_i^i$ are vectors expressed in the coordinate system, Σ_i. This means that R_i can calculate this inner product without referring to the static coordinate system, Σ_0. Therefore, R_i can determine its angular velocities of its wheels, $\dot{\phi}_{i1}$ and $\dot{\phi}_{i2}$, in Σ_i independently.

Consequently, the velocity of R_i is given as:

$$\begin{pmatrix} \dot{x}_i \\ \dot{y}_i \end{pmatrix} = M_i \begin{pmatrix} \tilde{v}_{xi} \\ \tilde{v}_{yi} \end{pmatrix}, \qquad M_i = \begin{pmatrix} \cos^2\theta_i(t) & \cos\theta_i(t)\sin\theta_i(t) \\ \sin\theta_i(t)\cos\theta_i(t) & \sin^2\theta_i(t) \end{pmatrix}. \tag{14}$$

As shown above, M_i is a symmetrical matrix and its eigenvalues are real and its eigenvectors which are perpendicular to each other span a two-dimensional space. We shall regard the vector, ${}^t(\tilde{v}_{xi}, \tilde{v}_{yi})$, in the right-hand side of Eq. (14) as a vector field and we shall express it as a linear combination of the eigenvectors of M_i as:

$$\begin{pmatrix} \tilde{v}_{xi} \\ \tilde{v}_{yi} \end{pmatrix} = a_{i1}\boldsymbol{w}_{i1} + a_{i2}\boldsymbol{w}_{i2},$$

where $\boldsymbol{w}_{i1}$ and $\boldsymbol{w}_{i2}$ are the eigenvectors of M_i. Then, Eq. (14) is rewritten as:

$$\begin{pmatrix} \dot{x}_i \\ \dot{y}_i \end{pmatrix} = M_i(a_{i1}\boldsymbol{w}_{i1} + a_{i2}\boldsymbol{w}_{i2}) = a_{i1}\lambda_{i1}\boldsymbol{w}_{i1} + a_{i2}\lambda_{i2}\boldsymbol{w}_{i2},$$

where λ_{i1} and λ_{i2} are the eigenvalues of M_i. We can see that the right-hand side of the above equation is a linear transformation of the vector field, $a_{i1}\boldsymbol{w}_{i1} + a_{i2}\boldsymbol{w}_{i2}$, by the matrix, M_i. The parameter, a_{i1}, expresses the direction and the magnitude of a flow along $\boldsymbol{w}_{i1}$ in this vector field. Since the trace of this matrix is positive and its determinant is zero independently of $\theta_i(t)$, i.e., independently of the rotation of R_i, the matrix has a positive eigenvalue and a zero-eigenvalue. This zero-eigenvalue makes an equilibrium region (that is a line and that includes an equilibrium point of $\tilde{\boldsymbol{v}}_i$, $\tilde{\boldsymbol{v}}_i = 0$), e.g., if $\lambda_{i1} = 0$, λ_{i1} makes the vector field, $a_{i1}\boldsymbol{w}_{i1} + a_{i2}\boldsymbol{w}_{i2}$, lose a flow along $\boldsymbol{w}_{i1}$ and it makes the equilibrium region (line) that is parallel to $\boldsymbol{w}_{i1}$ in this linear transformation, while λ_{i2} that is positive does not change the direction of a flow along $\boldsymbol{w}_{i2}$ but changes the magnitude of the flow. Hence, unless the robot rotates, it is trapped by the equilibrium region where $\tilde{\boldsymbol{v}}_i \perp \boldsymbol{e}_i$, i.e., ${}^t(\dot{x}_i, \dot{y}_i) = {}^t(0, 0)$. Of course, we cannot conclude from Eq. (14) that the rotating robot can avoid being trapped. We can just conclude from Eq. (14) that the robots stop without capturing/enclosing TARGET at least when they do not rotate, because M_i is not a full-rank matrix.

However, we strongly emphasize here that, in the averaged system of Eq. (14) (which we discuss below), M_i turns into a full-rank matrix whose eigenvalues are positive when the robots rotate and we can see that they achieve this cooperative hunting behavior.

3.4. Theorem by Eckhaus/Sanchez-Palencia in averaging theory

The method of averaging is a powerful mathematical tool to derive a time-independent system which gives approximate solutions of a time-dependent system. The time-independent system itself is an averaged system of the time-dependent system. Using the theorem by Eckhaus/Sanchez-Palencia, more than making such approximation, we can examine stability of the time-dependent systems by analyzing their averaged systems. Of course, this is not in all cases but in some cases. We especially emphasize that this theorem is applicable to analyzing stability of this robotic system. We recall the theorem in this subsection. Let us consider the equation:

$$\dot{\boldsymbol{x}} = \epsilon \boldsymbol{f}(t, \boldsymbol{x}), \quad \boldsymbol{x}(0) = \boldsymbol{x}_0,$$

where $\boldsymbol{x}_0, \boldsymbol{x} \in D \subset \mathbf{R}^n$; $\boldsymbol{f}(t, \boldsymbol{x}) : \mathbf{R}^+ \times \mathbf{R}^n \to \mathbf{R}^n$ is Lipschitz-continuous in $\boldsymbol{x}$ on $D \subset \mathbf{R}^n$, $t \geq 0$, and it is continuous in t and $\boldsymbol{x}$ on $\mathbf{R}^+ \times D$. If the average of $\boldsymbol{f}(t, \boldsymbol{x})$ over time,

$$\boldsymbol{f}^0(\boldsymbol{x}) = \lim_{T \to \infty} \frac{1}{T} \int_0^T \boldsymbol{f}(t, \boldsymbol{x})\, \mathrm{d}t,$$

exists, then $\boldsymbol{f}(t, \boldsymbol{x})$ is referred to as a *KBM* vector field. KBM stands for Krylov, Bogoliubov and Mitropolsky. We suppose that $\boldsymbol{f}(t, \boldsymbol{x})$ is a KBM vector field producing the averaged equation:

$$\dot{\boldsymbol{y}} = \epsilon \boldsymbol{f}^0(\boldsymbol{y}), \quad \boldsymbol{y}(0) = \boldsymbol{x}_0,$$

where $\boldsymbol{y}$ is an approximation of $\boldsymbol{x}$. When these five conditions: (i) $\boldsymbol{y} = \boldsymbol{y}_c$ is an asymptotically stable point in a linear approximation; (ii) $\boldsymbol{f}^0(\boldsymbol{y})$ is continuously differentiable with respect to $\boldsymbol{y}$ in D; (iii) $\boldsymbol{f}^0(\boldsymbol{y})$ has a domain of attraction, $D^0 \subset D$; (iv) $\boldsymbol{f}(t, \boldsymbol{y}_c) = 0$, and (v) $\boldsymbol{x}_0 \in D^0 \subset D$ hold, both $\boldsymbol{x}$ and $\boldsymbol{y}$ converge to $\boldsymbol{y}_c$ and the error between $\boldsymbol{x}$ and $\boldsymbol{y}$ is bounded as

$$\boldsymbol{x}(t) - \boldsymbol{y}(t) = \boldsymbol{O}(\delta(\epsilon)), \quad 0 \leq t < \infty,$$

where $\delta(\epsilon) = o(1)$.

In the following, we average this robotic system in Eq. (14) over time and we derive its averaged system which is just a first-order linear time-differential equation and which reflects stability of the robotic system in Eq. (14) as the case of the theorem of Eckhaus/Sanchez-Palencia and whose stability is described similarly as stability analysis of the desired system given in Section 3.2.

3.5. Averaged system

As we have described in Section 3.3, we design the orientations of the robots to be functions of time, which means that this robotic system is a time-dependent system. Not in all cases but in some cases, we can examine stability of time-dependent systems by analyzing their averaged systems that are time-independent. We especially emphasize that we can see stability of this robotic system in its averaged system as shown below.

The averaged system of Eq. (14) is given as:

$$\begin{pmatrix} \dot{X}_i \\ \dot{Y}_i \end{pmatrix} = \hat{M}_i \begin{pmatrix} \tilde{V}_{xi} \\ \tilde{V}_{yi} \end{pmatrix}, \tag{15}$$

$$\hat{M}_i = \lim_{T\to\infty}\frac{1}{T}\int_0^T M_i\,\mathrm{d}t = \begin{pmatrix} m_{i1} & m_{i2} \\ m_{i2} & m_{i3} \end{pmatrix},$$

$$m_{i1} = \lim_{T\to\infty}\frac{1}{T}\int_0^T \cos^2\theta_i(t)\,\mathrm{d}t,$$

$$m_{i2} = \lim_{T\to\infty}\frac{1}{T}\int_0^T \cos\theta_i(t)\sin\theta_i(t)\,\mathrm{d}t,$$

$$m_{i3} = \lim_{T\to\infty}\frac{1}{T}\int_0^T \sin^2\theta_i(t)\,\mathrm{d}t,$$

$$\begin{pmatrix} \tilde{V}_{xi} \\ \tilde{V}_{yi} \end{pmatrix} = \sum_{j\in \mathrm{L}_i}\tau_{ij}\left\{\begin{pmatrix} X_j \\ Y_j \end{pmatrix} - \begin{pmatrix} X_i \\ Y_i \end{pmatrix}\right\} + \tau_i\left\{\begin{pmatrix} x_t \\ y_t \end{pmatrix} - \begin{pmatrix} X_i \\ Y_i \end{pmatrix}\right\} + \begin{pmatrix} d_{xi} \\ d_{yi} \end{pmatrix}$$
$$+ \sum_{j\in\mathrm{OBJECTS}}\delta_{ij}\left[\left\{\begin{pmatrix} X_j \\ Y_j \end{pmatrix} - \begin{pmatrix} X_i \\ Y_i \end{pmatrix}\right\} - D\left\{\begin{pmatrix} X_j \\ Y_j \end{pmatrix} - \begin{pmatrix} X_i \\ Y_i \end{pmatrix}\right\}\Big/\left|\begin{pmatrix} X_j \\ Y_j \end{pmatrix} - \begin{pmatrix} X_i \\ Y_i \end{pmatrix}\right|\right],$$

$$\delta_{ij} = \begin{cases} \delta & |{}^t(X_j, Y_j) - {}^t(X_i, Y_i)| \le D, \\ 0 & |{}^t(X_j, Y_j) - {}^t(X_i, Y_i)| > D, \end{cases} \qquad j \in \mathrm{OBJECTS} = \mathrm{L}_i \cup \mathrm{M}_i \cup \mathrm{N}_i \cup \mathrm{TARGET},$$

$${}^t(X_i(0), Y_i(0)) = {}^t(x_i(0), y_i(0)),$$

where ${}^t(X_i, Y_i)$ is an approximation of ${}^t(x_i, y_i)$. Approximation errors in averaging theory are generally bounded only in finite time. However, if an averaged system (which is Eq. (15) here) has an attractor globally and an original system (which is Eq. (14) here) equilibrates on this attractor, i.e., if ${}^t(X_i, Y_i)$ converges to the attractor that we denote with ${}^t(X_{0i}, Y_{0i})$ and ${}^t(\dot{x}_i, \dot{y}_i) = {}^t(0, 0)$ holds in Eq. (14) where ${}^t(x_i, y_i) = {}^t(X_{0i}, Y_{0i})$, both ${}^t(X_i, Y_i)$ and ${}^t(x_i, y_i)$ converge to the attractor, ${}^t(X_{0i}, Y_{0i})$, and an error between them is bounded in $t \in [0, \infty]$ (see Eckhaus/Sanchez-Palencia's theorem [34, p. 70]).

As we can see in Eq. (15), the averaged system is identically the same as the desired system where ${}^t(\dot{x}_i, \dot{y}_i) = {}^t(\tilde{v}_{xi}, \tilde{v}_{yi})$ holds except that the vector field, ${}^t(\tilde{V}_{xi}, \tilde{V}_{yi})$, is transformed by the matrix, $\hat{M}_i$, which is symmetric. If both the eigenvalues of the matrix, $\hat{M}_i$, are positive, the orientations of the flows of the vector field are invariant while the magnitudes of the flows are changed in this linear transformation. This means that, if so, the averaged system and the desired system have the same attractor where the robots (which are holonomic mobile robots) capture/enclose TARGET by making troop formations (see [43,47]), i.e., where ${}^t(\tilde{v}_{xi}, \tilde{v}_{yi}) = {}^t(0, 0)$ holds. Of course, the original system (this robotic system) equilibrates on this attractor, because ${}^t(\dot{x}_i, \dot{y}_i) = {}^t(0, 0)$ holds in Eq. (14) where ${}^t(\tilde{v}_{xi}, \tilde{v}_{yi}) = {}^t(0, 0)$. This deduces the fact that, if both the eigenvalues of $\hat{M}_i$ are positive, the robots (which are nonholonomic mobile robots of the Hilare-type in the original system, i.e., in this robotic system) also capture/enclose TARGET the same as the case of the desired system and they certainly achieve this cooperative behavior. Therefore, in the following, we examine the eigenvalues of the matrix, $\hat{M}_i$.

Similarly in the case of Eq. (14), the right-hand side of Eq. (15) is a linear transformation of the vector field, ${}^t(\tilde{V}_{xi}, \tilde{V}_{yi})$, by the matrix, $\hat{M}_i$. As we have described, the robots stop without capturing/enclosing TARGET at least when they do not rotate, because M_i in Eq. (14) is not a full-rank matrix. This must also hold in Eq. (15), since it is an approximation of Eq. (14). Obviously, the trace of $\hat{M}_i$ is positive independently of $\theta_i(t)$, i.e., independently of the rotation of R_i. The determinant of $\hat{M}_i$ is given as:

$$\det\hat{M}_i = \left(\frac{1}{T}\int_0^T \cos^2\theta_i(t)\,\mathrm{d}t\right)\left(\frac{1}{T}\int_0^T \sin^2\theta_i(t)\,\mathrm{d}t\right) - \left(\frac{1}{T}\int_0^T \cos\theta_i(t)\sin\theta_i(t)\,\mathrm{d}t\right)^2, \quad T\to\infty.$$

When the robot, R_i, does not rotate, $\det \hat{M}_i = 0$ holds and we conclude that the robot fails to achieve this cooperative hunting behavior. To show the range that $\det \hat{M}_i$ takes, we use the following theorem in functional analysis.

Theorem. *Let $1 < p < \infty$ and let $1/p + 1/q = 1$ and then we have*

$$\int_a^b |f(t)g(t)|\,\mathrm{d}t \le \left(\int_a^b |f(t)|^p\,\mathrm{d}t\right)^{1/p}\left(\int_a^b |g(t)|^q\,\mathrm{d}t\right)^{1/q},$$

where $f(t)$, $g(t)$ and $f(t)g(t)$ are Lebesgue integrable. The range of this integral can be infinite. This inequality is referred to as "Hölder's inequality" (*see* [51, p. 33]).

Remark. The equality sign in this inequality holds if and only if there exists a non-negative constant c such that $|f(t)| = c|g(t)|^{1/(p-1)}$.

Let $p = q = 2$ and let us modify this inequality as:

$$\left|\int_a^b f(t)g(t)\,\mathrm{d}t\right| \le \int_a^b |f(t)g(t)|\,\mathrm{d}t \le \left(\int_a^b |f(t)|^2\,\mathrm{d}t\right)^{1/2}\left(\int_a^b |g(t)|^2\,\mathrm{d}t\right)^{1/2}$$

and

$$\left(\int_a^b f(t)g(t)\,\mathrm{d}t\right)^2 \le \left(\int_a^b f(t)^2\,\mathrm{d}t\right)\left(\int_a^b g(t)^2\,\mathrm{d}t\right)$$

and then we derive

$$\left(\frac{1}{T}\int_0^T \cos\theta_i(t)\sin\theta_i(t)\,\mathrm{d}t\right)^2 \le \left(\frac{1}{T}\int_0^T \cos^2\theta_i(t)\,\mathrm{d}t\right)\left(\frac{1}{T}\int_0^T \sin^2\theta_i(t)\,\mathrm{d}t\right), \quad T \to \infty.$$

If and only if the robot does not rotate, there exists a constant c such that $\cos\theta_i(t) = c\sin\theta_i(t)$ and the equality sign of the above inequality holds, i.e., $\det \hat{M}_i = 0$ holds as $\det M_i = 0$. However, if the robot rotates, $\det \hat{M}_i > 0$ holds and $\hat{M}_i$ is a full-rank matrix whose eigenvalues are positive and then it follows that the robots capture/enclose TARGET by making troop formations. In other words, the averaged system explicitly describes both the cases where the non-rotating robots cannot achieve this cooperative hunting behavior and where the rotating robots can do so, while the original system (which is Eq. (14)) explicitly describes only the former case. Hence, we conclude that we can see stability of this type of nonholonomic mechanical system which consists of multiple nonholonomic mobile robots of the Hilare-type in its averaged system. We particularly emphasize that $\det \hat{M}_i \ge 0$ is the "most important mathematical formula" in this mechanical system, because this formula gives us a clue to examine stability that we cannot see in the original system. Of course, each robot is not required to keep rotating. The robot can stop its rotating motion and it can direct its orientation in its desired direction, after $\tilde{\boldsymbol{v}}_i = 0$ holds, i.e., after it captures/encloses TARGET by making troop formations with other robots. Even if the robots do not synchronize their rotating motions, they achieve this cooperative hunting behavior. Since we can choose any non-constant time-varying function as $\theta_i(t)$, this control law allows for wide variety of time-varying feedback.

We summarize the point of this section here. Based on Eckhaus/Sanchez-Palencia's theorem (see [34, p. 70]), in averaging theory, we have proven that the convergence value of ${}^t(x_i, y_i)$ in the desired system where each robot is a holonomic mobile robot actually gives the final position of R_i which is a nonholonomic mobile robot of the Hilare-type, when the robot rotates. Therefore, we can derive the final relative position of the troop to TARGET and the final formation of the troop, by analyzing the desired system that is just a first-order linear time-differential equation and that is independent of the rotating motions of the robots. In the following, we formulate how the robots capture/enclose TARGET by making troop formations.

4. Formation control

4.1. Relative positions to TARGET

To capture/enclose TARGET, the troop needs to have an appropriate relative position to TARGET and the troop also needs to make an appropriate formation around it. In this subsection, we describe how the final relative position is determined in the desired system where each robot is a holonomic mobile robot. Of course, each robot in this control law has a nonholonomic constraint. However, as we have described, when the robot rotates, the original system (this robotic system in Eq. (14)) and the desired system have the same attractor where the robots (which are holonomic mobile robots) capture/enclose TARGET (see [43,47]), so that, by analyzing the desired system that is just a first-order linear time-differential equation and that is independent of the rotating motions of the robots, we can derive the final relative position of the troop to TARGET and the final formation of the troop in the original system where each robot is a nonholonomic mobile robot of the Hilare-type. In the following, we expand mathematical formulas describing the desired system in order to derive the final relative position of the troop to TARGET. The (n) relative positions of the (n) robots to TARGET are given as:

$$ {}^t(\theta_{xi}, \theta_{yi}) = {}^t(x_i, y_i) - {}^t(x_t, y_t), \tag{16} $$

where $i = 1, 2, \dots, n$. From Eqs. (4) and (16), using $\boldsymbol{B}\boldsymbol{v}_1 = 0$ and $\boldsymbol{C}\boldsymbol{v}_1 = 0$, the time-differentials of the relative positions in the desired system are derived as:

$$ \begin{pmatrix} \dot{\boldsymbol{\theta}}_x \\ \dot{\boldsymbol{\theta}}_y \end{pmatrix} = \begin{pmatrix} B + C - \Delta - \Lambda & 0 \\ 0 & B + C - \Delta - \Lambda \end{pmatrix} \begin{pmatrix} \boldsymbol{\theta}_x \\ \boldsymbol{\theta}_y \end{pmatrix} - \begin{pmatrix} \Lambda & 0 \\ 0 & \Lambda \end{pmatrix} \begin{pmatrix} x_t \boldsymbol{v}_1 \\ y_t \boldsymbol{v}_1 \end{pmatrix} - \begin{pmatrix} \dot{x}_t \boldsymbol{v}_1 \\ \dot{y}_t \boldsymbol{v}_1 \end{pmatrix} + \begin{pmatrix} \boldsymbol{d}_x \\ \boldsymbol{d}_y \end{pmatrix} + \begin{pmatrix} \boldsymbol{\xi}_x \\ \boldsymbol{\xi}_y \end{pmatrix}, \tag{17} $$

$$ \boldsymbol{\theta}_x = {}^t(\theta_{x1}, \theta_{x2}, \dots, \theta_{xn}), \qquad \boldsymbol{\theta}_y = {}^t(\theta_{y1}, \theta_{y2}, \dots, \theta_{yn}). $$

When any relative distance of any robot to any other robot, any obstacle and TARGET is longer than D, any repulsion (which repulses a robot from the other robots, the obstacles and TARGET for collision avoidance) does not work and the relative positions calculated below are exactly the same as the final relative positions of the robots (which are nonholonomic mobile robots of the Hilare-type) to TARGET. Even if the repulsion works, we can estimate the final relative positions, since the repulsion works only in the limited areas around the robots, the obstacles and TARGET. In the following, we calculate the relative positions only in cases where any repulsion does not work. In such cases, $\delta_{ij} = 0$, $i = 1, 2, \dots, n$, $j \in$ OBJECTS, holds and Eq. (17) is written as:

$$ \begin{pmatrix} \dot{\boldsymbol{\theta}}_x \\ \dot{\boldsymbol{\theta}}_y \end{pmatrix} = \begin{pmatrix} B - \Delta & 0 \\ 0 & B - \Delta \end{pmatrix} \begin{pmatrix} \boldsymbol{\theta}_x \\ \boldsymbol{\theta}_y \end{pmatrix} + \begin{pmatrix} \boldsymbol{d}_x \\ \boldsymbol{d}_y \end{pmatrix} - \begin{pmatrix} \dot{x}_t \boldsymbol{v}_1 \\ \dot{y}_t \boldsymbol{v}_1 \end{pmatrix}, \tag{18} $$

where ${}^t(\dot{x}_t, \dot{y}_t)$ is the velocity of TARGET. Since we suppose the troop to pursue TARGET in closed environments, e.g., in buildings, TARGET possibly loses its escape route and it is finally captured/enclosed by the troop. In the case where TARGET slows down and ${}^t(\dot{x}_t, \dot{y}_t) = {}^t(0, 0)$ holds, the convergence value of ${}^t({}^t\boldsymbol{\theta}_x, {}^t\boldsymbol{\theta}_y)$ is given as:

$$ \begin{pmatrix} \boldsymbol{\theta}_x \\ \boldsymbol{\theta}_y \end{pmatrix} = \begin{pmatrix} -(B - \Delta)^{-1} & 0 \\ 0 & -(B - \Delta)^{-1} \end{pmatrix} \begin{pmatrix} \boldsymbol{d}_x \\ \boldsymbol{d}_y \end{pmatrix}. \tag{19} $$

Moreover, when all the robots can sense their relative positions to TARGET, $\Delta = \tau I_n$ holds and Eq. (19) is rewritten as:

$$\begin{pmatrix} \boldsymbol{\theta}_x \\ \boldsymbol{\theta}_y \end{pmatrix} = \begin{pmatrix} -(B-\tau I_n)^{-1} & 0 \\ 0 & -(B-\tau I_n)^{-1} \end{pmatrix} \begin{pmatrix} \boldsymbol{d}_x \\ \boldsymbol{d}_y \end{pmatrix}, \tag{20}$$

where I_n is a $n \times n$ identity matrix. This equation means that the final relative position of the troop to TARGET and the final formation of the troop are determined solely by the formation vectors, ${}^t(d_{xi}, d_{yi})$, $i = 1, 2, \ldots, n$. In Section 4.3, we discuss the determination of the formation vectors for capturing/enclosing TARGET.

As we have assumed in Section 3.1, at least one mobile robot in the troop can sense its relative position to TARGET and the robot is attracted to it by the second term in the right-hand side of Eq. (1). Since the troop has a strongly connected configuration, other robots are pulled by the robot toward TARGET and all the robots can finally sense their relative positions to TARGET. Of course, in some cases, obstacles prevent some robots from sensing TARGET and the troop gets stuck, which is referred to as a deadlock. Solving deadlocks will be investigated in future work.

4.2. Troop formation

To describe troop formations, we define $(n-1)$ relative position vectors between the (n) robots as:

$${}^t(\phi_{xk}, \phi_{yk}) = {}^t(x_j - x_i, y_j - y_i), \tag{21}$$

where $k = 1, 2, \ldots, n-1$. These vectors are required to form a connected oriented-graph (in which a robot is a node and a relative position vector is an oriented path between the robots and in which all the (n) nodes are connected together by the $(n-1)$ oriented paths), otherwise they cannot describe formations uniquely. To handle all the x-components and all the y-components of the relative position vectors separately, we define two vectors as:

$$\boldsymbol{\phi}_x = {}^t(\phi_{x1}, \phi_{x2}, \ldots, \phi_{xn-1}), \qquad \boldsymbol{\phi}_y = {}^t(\phi_{y1}, \phi_{y2}, \ldots, \phi_{yn-1}).$$

The vectors, $\boldsymbol{\phi}_x$ and $\boldsymbol{\phi}_y$, are related with $\boldsymbol{x}$ and $\boldsymbol{y}$ as:

$$\begin{pmatrix} \boldsymbol{\phi}_x \\ \boldsymbol{\phi}_y \end{pmatrix} = \begin{pmatrix} P & 0 \\ 0 & P \end{pmatrix} \begin{pmatrix} \boldsymbol{x} \\ \boldsymbol{y} \end{pmatrix}, \qquad P = \begin{pmatrix} \boldsymbol{f}_1 \\ \boldsymbol{f}_2 \\ \vdots \\ \boldsymbol{f}_{n-1} \end{pmatrix}, \qquad \boldsymbol{f}_i = (\ldots, 1, \ldots, -1, \ldots), \quad i < n,$$

where $P \in \mathbf{R}^{(n-1)\times n}$ and $\boldsymbol{f}_i \in \mathbf{R}^{1\times n}$. All the components of $\boldsymbol{f}_i$ are zero except two of them: 1 and -1. The $\boldsymbol{f}_i$'s are linearly independent of each other, which means that the relative position vectors form a connected oriented-graph mentioned above. Here, we give an example of P as follows.

$$P = \begin{pmatrix} 1 & 0 & \cdots & 0 & -1 \\ 0 & 1 & \ddots & \vdots & -1 \\ \vdots & \ddots & \ddots & 0 & \vdots \\ 0 & \cdots & 0 & 1 & -1 \end{pmatrix}.$$

When any relative distance of any robot to any other robot, any obstacle and TARGET is longer than D, $\delta_{ij} = 0$, $i = 1, 2, \ldots, n$, $j \in$ OBJECTS, holds. Moreover, when all the robots can sense their relative positions to TARGET, using $\boldsymbol{\phi}_x = P\boldsymbol{x} = P\boldsymbol{\theta}_x$ and $\boldsymbol{\phi}_y = P\boldsymbol{y} = P\boldsymbol{\theta}_y$, the convergence value of $\boldsymbol{\phi}_x$ and $\boldsymbol{\phi}_y$ are derived from Eq. (20) as:

$$\begin{pmatrix} \boldsymbol{\phi}_x \\ \boldsymbol{\phi}_y \end{pmatrix} = \begin{pmatrix} -P(B-\tau I_n)^{-1} & 0 \\ 0 & -P(B-\tau I_n)^{-1} \end{pmatrix} \begin{pmatrix} \boldsymbol{d}_x \\ \boldsymbol{d}_y \end{pmatrix}. \quad (22)$$

The above equation, Eq. (22), means that $\boldsymbol{\phi}_x$ and $\boldsymbol{\phi}_y$ are determined solely by ${}^t(d_{xi}, d_{yi})$, $i = 1, 2, \ldots, n$, i.e., the final formation is determined solely by the formation vectors. Since P is full-rank and $(B - \tau I_n)$ is asymptotically stable, the formation is controllable by ${}^t(d_{xi}, d_{yi})$, $i = 1, 2, \ldots, n$. Let us refer to this controllability as *formation controllability*.

4.3. Determination of formation vectors

As we have described, the final relative position of the troop to TARGET and the final formation of the troop are controllable by the formation vectors independently of the rotating motions of the robots, when all the robots sense TARGET and at the same time TARGET is static losing its escape route in closed environments, e.g., in buildings. This means that the formation vectors are control inputs for capturing/enclosing TARGET by making troop formations. In this subsection, we give two examples of the determination of the formation vector and these are used to capture/enclose TARGET by making an arc-like formation in computer simulations later. We suppose R_i to determine its formation vector, ${}^t(d_{xi}, d_{yi})$, in Σ_i. More specifically, we suppose R_i to determine ${}^t(d_{xi}, d_{yi})$ according to its surrounding environment in Σ_i, e.g., according to its relative position to $R_j \in L_i$ and TARGET in Σ_i. Fig. 4(a) shows that R_i directs ${}^t(d_{xi}, d_{yi})$ along the line passing the origin of Σ_i from TARGET. Fig. 4(b) shows that R_i directs ${}^t(d_{xi}, d_{yi})$ along the line that is passing the origin of Σ_i and that is perpendicular to the line between TARGET and R_j. Fig. 4(a) physically means that R_i tries to keep a relative position to TARGET that is parallel to ${}^t(d_{xi}, d_{yi})$. We can also describe the physical meaning of Fig. 4(b) similarly. These determinations are regarded as reactions of a robot according to its surrounding environment. Therefore, we can see that each robot determines its formation vector in a reactive control framework.

Since both the formation vectors in Fig. 4(a) and (b) are independent of Σ_i, they are invariant even if R_i changes its orientation. In other words, formation controllability is invariant under the rotation of R_i. We can, of course, consider the formation vector, ${}^t(d_{xi}, d_{yi})$, to depend on Σ_i. In such cases, the orientation of R_i is one of formation control elements. This will be investigated in future work. Thus, we are considering two mappings: one is S_i, a mapping from the surrounding environment of R_i to ${}^t(d_{xi}, d_{yi})$, and the other is T, a mapping from ${}^t(d_{xi}, d_{yi})$, $i = 1, 2, \ldots, n$, to the formation (see Fig. 5). The determinations of ${}^t(d_{xi}, d_{yi})$ in Fig. 4(a) and (b) are examples of S_i. We can design others of S_i. However, we cannot always guarantee to find an appropriate design of S_i for each application, because R_i determines ${}^t(d_{xi}, d_{yi})$ only according to its own surrounding environment and its determination is independent of others'. Hence, although, as we have described, the formation is controllable by ${}^t(d_{xi}, d_{yi})$, $i = 1, 2, \ldots, n$,

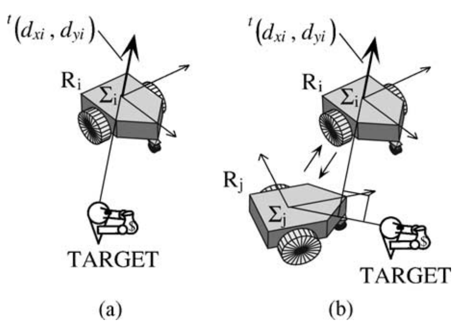

Fig. 4. Determination of ${}^t(d_{xi}, d_{yi})$.

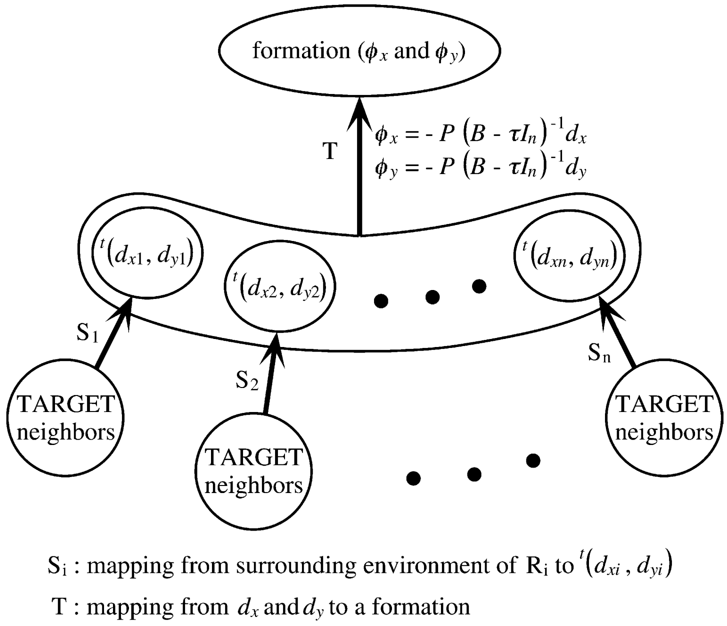

Fig. 5. Mappings, S_i and T, in making formations.

we cannot say that it is possible to make any formation, as long as R_i determines its formation vector, ${}^t(d_{xi}, d_{yi})$, independently.

From Eq. (22), using $(B - \tau I_n)\boldsymbol{v}_1 = -\tau \boldsymbol{v}_1 \in \mathrm{Ker}(B)$, the inverse mapping of T is derived as:

$$\begin{pmatrix} \boldsymbol{d}_x \\ \boldsymbol{d}_y \end{pmatrix} = \begin{pmatrix} -(B - \tau I_n)\,{}^tP(P\,{}^tP)^{-1} & 0 \\ 0 & -(B - \tau I_n)\,{}^tP(P\,{}^tP)^{-1} \end{pmatrix} \begin{pmatrix} \boldsymbol{\phi}_x \\ \boldsymbol{\phi}_y \end{pmatrix} - \tau \begin{pmatrix} h_x \boldsymbol{v}_1 \\ h_y \boldsymbol{v}_1 \end{pmatrix}, \tag{23}$$

where h_x and h_y are arbitrary scalars, because $\boldsymbol{d}_x$ and $\boldsymbol{d}_y$ are (n)-dimensional vectors while $\boldsymbol{\phi}_x$ and $\boldsymbol{\phi}_y$ are $(n-1)$-dimensional vectors. Substituting the right-hand side in Eq. (23) for ${}^t({}^t\boldsymbol{d}_x, {}^t\boldsymbol{d}_y)$ in Eq. (20), we rewrite the (n) relative positions of the (n) robots to TARGET as:

$$\begin{pmatrix} \boldsymbol{\theta}_x \\ \boldsymbol{\theta}_y \end{pmatrix} = \begin{pmatrix} {}^tP(P\,{}^tP)^{-1} & 0 \\ 0 & {}^tP(P\,{}^tP)^{-1} \end{pmatrix} \begin{pmatrix} \boldsymbol{\phi}_x \\ \boldsymbol{\phi}_y \end{pmatrix} - \begin{pmatrix} h_x \boldsymbol{v}_1 \\ h_y \boldsymbol{v}_1 \end{pmatrix}. \tag{24}$$

As Eq. (24) shows, even if we determine the formation, $\boldsymbol{\phi}_x$ and $\boldsymbol{\phi}_y$, the relative position of the troop to TARGET is not unique. The relative position depends on ${}^t(h_x, h_y)$. Since $\boldsymbol{\phi}_x$, $\boldsymbol{\phi}_y$ and ${}^t(h_x, h_y)$ are determined by the formation vectors as Eq. (23) shows, we have to design the formation vectors in order for the troop to have an appropriate relative position to TARGET and to make an appropriate formation around it.

4.4. Other formations

It is possible to make other formations using this control law. As we have described, the formation vector of R_i physically means that the robot, R_i, is pulled in the direction of the vector. The pulling strength is proportional to the norm of the vector. To elaborate the relation between the robot and formation control, let us consider the following three simple cases where we control the relative positions between the robots to make some formations without having the attraction to TARGET, i.e., without sensing TARGET. In the first case where we control the relative position between two robots sensing each other along a specified line, e.g., along the x-axis, we need to set the directions of their formation vectors to be opposite to each other along the specified line and we also need to adjust the norms of the vectors. In the second case where we make a straight-line formation of multiple robots in an open chain configuration along a specified line at even intervals, the formation vectors of the non-end robots cancel out each other and these vectors are zero-formation vectors when all the attraction coefficients between the robots are the same while the formation vectors of the end robots have the directions opposite to each other along the specified line and their norms are the same. The length of the straight-line formation is proportional to the norms of the formation vectors of the end robots. In the third case where we make a triangle-formation, the robots in an open chain configuration are regarded as a string, and both the end robots and the robots in the middle of the configuration are pulled by their formation vectors. The size of the triangle-formation is proportional to the norms of the vectors. Of course, the robots are attracted to TARGET when they sense it, so that we have to adjust the formation vectors to compensate the deformation by the attraction. The formation vectors required to make some specified formation of the troop around TARGET and required to make some specified relative position of the troop to TARGET are calculated by Eq. (20). In Section 5, we show a simulation result in Fig. 14 where the robots make a triangle-formation around TARGET. The formation vectors for this triangle-formation are calculated by Eq. (20).

5. Simulations

We simulated this cooperative behavior as shown in Fig. 6. A robot troop consists of eight nonholonomic mobile robots of the Hilare-type. Each robot can recognize whether it is an end or not in this troop, because an end robot senses only one robot while a non-end robot senses two robots. We give rules (reactions) to determine the formation vectors as: (i) a non-end robot has ${}^t(d_{xi}, d_{yi})$ in Fig. 4(a); (ii) a non-end robot has a zero-formation vector when it cannot see TARGET; (iii) an end robot has ${}^t(d_{xi}, d_{yi})$ in Fig. 4(b), and (iv) an end robot has a zero-formation vector when it cannot see TARGET. In Fig. 6, R_1 which is an end robot has ${}^t(d_{xi}, d_{yi})$ in Fig. 4(b) and R_2 which is a non-end has ${}^t(d_{xi}, d_{yi})$ in Fig. 4(a). We set the formation vector norms as: $|{}^t(d_{xi}, d_{yi})| = 3.0$, $i = 1, 2, \dots, 8$, and the attraction coefficient of R_i to R_j as: $\tau_{ij} = \tau_{ji} = 4.0$, $i = 1, 2, \dots, 7$, $j = i + 1$. We also set the parameters as: $\tau = 1.0$; $\delta = 200.0$, and $D = 0.3$ m. Each R_i in the simulations rotates its orientation as: (i) $\dot{\theta}_i(t) = 2.0\pi/2.5$ rad/s in Figs. 7, 11–14; (ii) $\dot{\theta}_i(t) = -2.0\pi/2.5$ rad/s in Fig. 8; (iii) $\dot{\theta}_i(t) = k_i\{(\theta_0 + A_0 \sin \omega_i t) - \theta_i(t)\}$ rad/s, $k_i = 4.0$, $\theta_0 = -\pi/2.0$ rad, $A_0 = \pi$ rad, and $\omega_i = 2.0\pi/2.5$ rad/s in Fig. 9; (iv) $\dot{\theta}_i(t) = k_i\{(\theta_0 + A_i \sin \omega_i t) - \theta_i(t)\}$ rad/s,

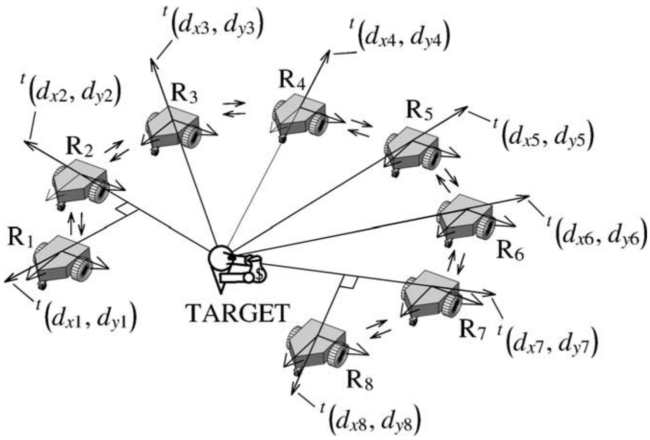

Fig. 6. A mobile robot troop.

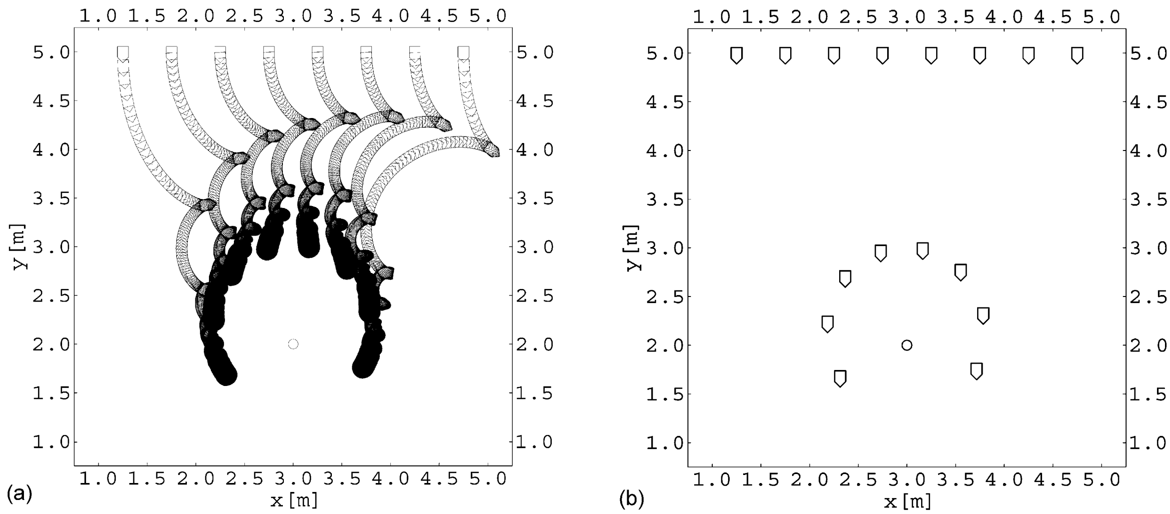

Fig. 7. Evolutions of robot positions and orientations. (a) $t = 0.0$–30.0 s; (b) $t = 0.0, 30.0$ s.

$k_i = 4.0$, $\theta_0 = -\pi/2.0$ rad, $A_i = \pi$ rad when $g_i|\tilde{\boldsymbol{v}}_i| \geq \pi$, $A_i = g_i|\tilde{\boldsymbol{v}}_i|$ rad when $g_i|\tilde{\boldsymbol{v}}_i| < \pi$, $g_i = 10.0$, and $\omega_i = 2.0\pi/2.5$ rad/s in Fig. 10. The case of (i) physically means that the robot rotates counterclockwise at the angular velocity, $2.0\pi/2.5$ rad/s. The case of (ii) means that the robot rotates clockwise at the angular velocity, $-2.0\pi/2.5$ rad/s. The case of (iii) means that the robot oscillates its orientation around the angle, $-\pi/2.0$ rad. The case of (iv) means that the robot oscillates its orientation as the case of (iii), however, its oscillation amplitude approaches zero as the norm of its desired velocity, $|\tilde{\boldsymbol{v}}_i|$, converges to zero. In other words, each robot is not required to keep rotating/oscillating. The robot can stop its rotating/oscillating motion and it can direct its orientation in its desired direction, after $\tilde{\boldsymbol{v}}_i = 0$ holds, i.e., after it captures/encloses TARGET by making troop formations with other robots. Even if the robots do not synchronize their rotating/oscillating motions, they achieve this cooperative

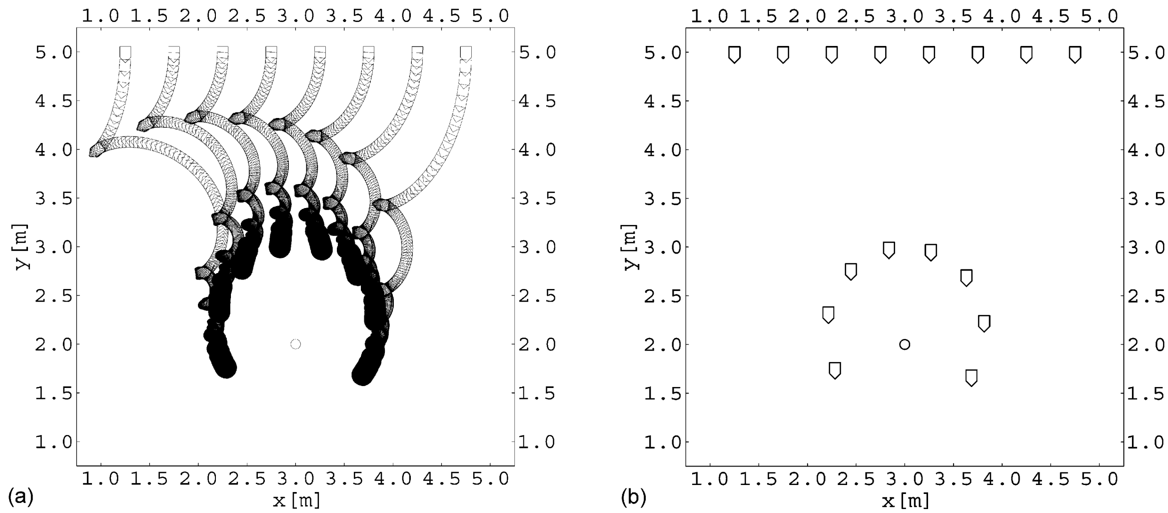

Fig. 8. Evolutions of robot positions and orientations. (a) $t = 0.0$–30.0 s; (b) $t = 0.0, 30.0$ s.

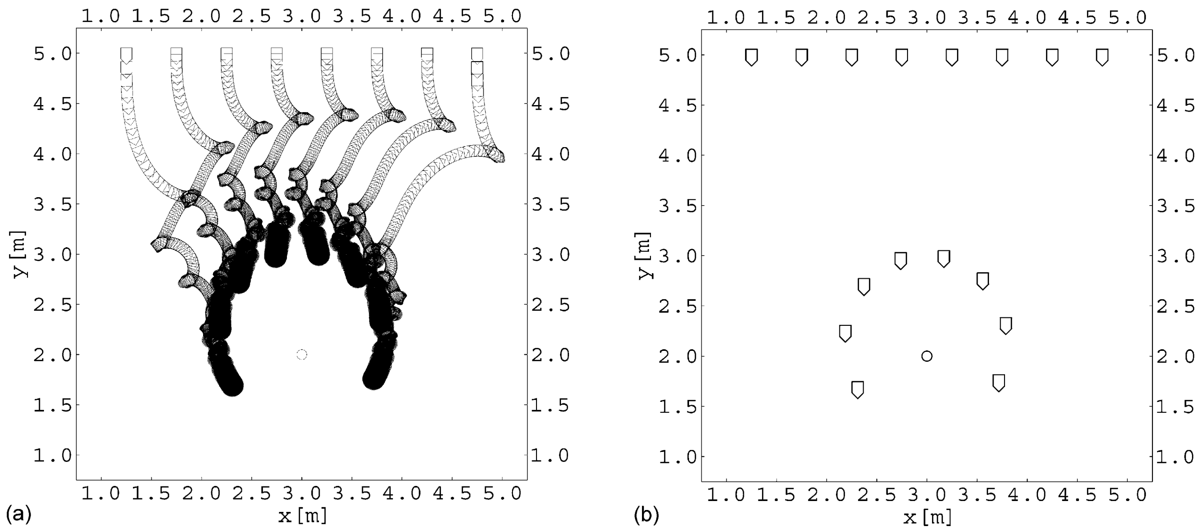

Fig. 9. Evolutions of robot positions and orientations. (a) $t = 0.0$–30.0 s; (b) $t = 0.0$, 30.2 s.

hunting behavior. Since we can choose any non-constant time-varying function as $\theta_i(t)$, this control law allows for wide variety of time-varying feedback.

Throughout all the simulations, all the robots are initially located on the line: $y = 5.0$ m at an interval of 0.5 m and the initial orientation of each R_i is set as: $\theta_i(0) = -\pi/2.0$ rad. Fig. 7(a) shows a simulation result where TARGET is static on the coordinate: ${}^t(3.0, 2.0)$ and where each R_i rotates as: $\dot{\theta}_i(t) = 2.0\pi/2.5$ rad/s. We can see that the rotating robots capture/enclose TARGET by making an arc-like formation. Collisions between the robots are avoided by the repulsion, the fourth term in Eq. (1). Fig. 7(b) shows the final relative positions of the robots to TARGET. Because the norms of the formation vectors are long enough to make any relative distance of any robot to any other robot

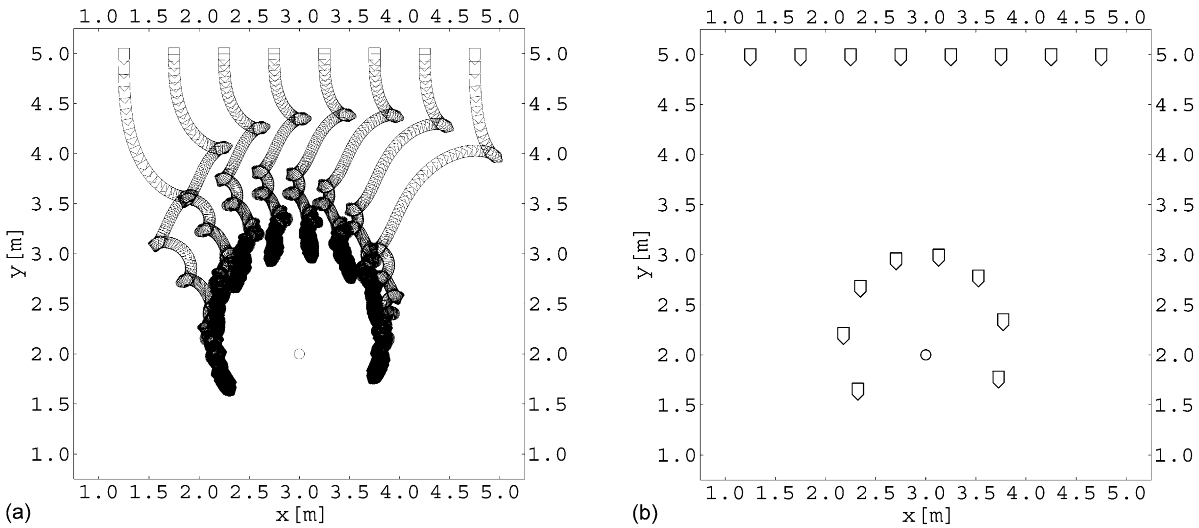

Fig. 10. Evolutions of robot positions and orientations. (a) $t = 0.0$–30.0 s; (b) $t = 0.0$, ∞ s.

and TARGET longer than $D = 0.3$ m, the repulsion, the fourth term in Eq. (1), does not work, and the final relative positions of the robots to TARGET are described by Eq. (20), which we can see as follows. The convergence values of the formation vectors are given as:

$$\boldsymbol{d_x} = {}^t(-0.86, -2.87, -1.99, -0.79, 0.49, 1.75, 2.77, 1.15), \tag{25}$$

$$\boldsymbol{d_y} = {}^t(-2.87, 0.86, 2.24, 2.89, 2.96, 2.43, 1.15, -2.77). \tag{26}$$

From Eqs. (20), (25) and (26), the final relative positions of the robots to TARGET are calculated as:

$$\boldsymbol{\theta_x} = {}^t(-0.69, -0.81, -0.63, -0.27, 0.17, 0.56, 0.79, 0.72), \tag{27}$$

$$\boldsymbol{\theta_y} = {}^t(-0.32, 0.24, 0.71, 0.97, 0.99, 0.77, 0.33, -0.25), \tag{28}$$

$$B = \begin{pmatrix} -4.0 & 4.0 & 0 & 0 & 0 & 0 & 0 & 0 \\ 4.0 & -8.0 & 4.0 & 0 & 0 & 0 & 0 & 0 \\ 0 & 4.0 & -8.0 & 4.0 & 0 & 0 & 0 & 0 \\ 0 & 0 & 4.0 & -8.0 & 4.0 & 0 & 0 & 0 \\ 0 & 0 & 0 & 4.0 & -8.0 & 4.0 & 0 & 0 \\ 0 & 0 & 0 & 0 & 4.0 & -8.0 & 4.0 & 0 \\ 0 & 0 & 0 & 0 & 0 & 4.0 & -8.0 & 4.0 \\ 0 & 0 & 0 & 0 & 0 & 0 & 4.0 & -4.0 \end{pmatrix}, \qquad \tau = 2.0.$$

We can see that the convergence values of $\boldsymbol{\theta_x}$ and $\boldsymbol{\theta_y}$ in Eqs. (27) and (28) exactly describe the final relative positions of the robots to TARGET in Fig. 7(b).

Fig. 8(a) and (b) show a simulation result where TARGET is static on the coordinate: ${}^t(3.0, 2.0)$ and where each R_i rotates as: $\dot{\theta}_i(t) = -2.0\pi/2.5$ rad/s. We can see that the troop achieves this cooperative behavior in this case.

Fig. 9(a) and (b) show a simulation result where TARGET is static on the coordinate: ${}^t(3.0, 2.0)$ and where each R_i oscillates its orientation as: $\dot{\theta}_i(t) = k_i\{(\theta_0 + A_0 \sin \omega_i t) - \theta_i(t)\}$ rad/s, $k_i = 4.0$, $\theta_0 = -\pi/2.0$ rad, $A_0 = \pi$ rad, and $\omega_i = 2.0\pi/2.5$ rad/s. We can see that the troop achieves this cooperative behavior in this case.

Fig. 10(a) and (b) show a simulation result where TARGET is static on the coordinate: ${}^t(3.0, 2.0)$ and where each R_i oscillates its orientation as: $\dot{\theta}_i(t) = k_i\{(\theta_0 + A_i \sin \omega_i t) - \theta_i(t)\}$ rad/s, $k_i = 4.0$, $\theta_0 = -\pi/2.0$ rad, $A_i = \pi$ rad when $g_i|\tilde{\boldsymbol{v}}_i| \geq \pi$, $A_i = g_i|\tilde{\boldsymbol{v}}_i|$ rad when $g_i|\tilde{\boldsymbol{v}}_i| < \pi$, $g_i = 10.0$, and $\omega_i = 2.0\pi/2.5$ rad/s. This means that each R_i reduces its oscillation amplitude as the norm of the desired velocity, $|\tilde{\boldsymbol{v}}_i|$, converges to zero. Each R_i finally stops its oscillating motion and it directs its orientation in the direction, $\theta_0 = -\pi/2.0$ rad. We can see that the troop also achieves this cooperative behavior in this case.

Fig. 11(a) and (b) show a simulation result where TARGET moves at the velocity, ${}^t(-0.1, -0.05)$ m/s, and its initial location is the coordinate: ${}^t(4.5, 3.2)$ and where each R_i rotates as: $\dot{\theta}_i(t) = 2.0\pi/2.5$ rad/s. The troop pursues TARGET. The relative distance of the troop to TARGET is proportional to the moving velocity of TARGET. When TARGET moves faster, the relative distance of the troop to TARGET becomes longer. When TARGET loses its escape route in closed environments, e.g., in building, and it slows down, the troop achieves this cooperative behavior.

Fig. 12(a) and (b) show a simulation result where TARGET is static on the coordinate: ${}^t(3.0, 2.0)$ and where each R_i rotates as: $\dot{\theta}_i(t) = 2.0\pi/2.5$ rad/s. We put a cylindrical obstacle whose center is located on the coordinate: ${}^t(2.0, 3.5)$ and whose radius is 0.5 m. Initially, the robots, R_1 and R_2, cannot see TARGET, so that they have zero-formation vectors. However, since R_2 is attracted to R_3 by the first term in the right-hand side of Eq. (1), it approaches TARGET. Similarly, R_1 is attracted to R_2 and it also approaches TARGET. Finally, all the robots can see TARGET and they achieve this cooperative behavior in this case.

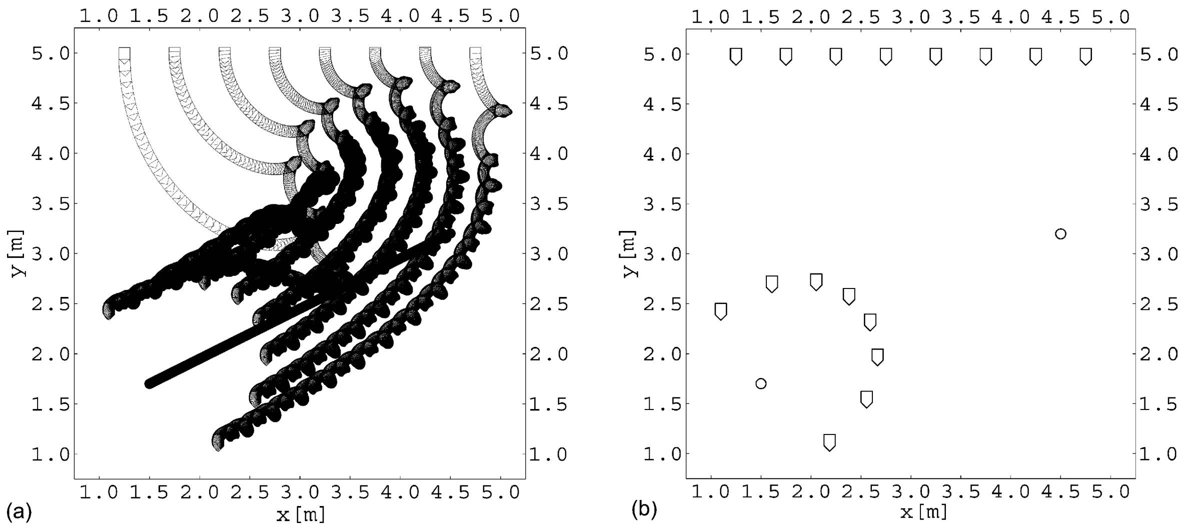

Fig. 11. Evolutions of robot positions and orientations. (a) $t = 0.0$–30.0 s; (b) $t = 0.0, 30.0$ s.

Fig. 13(a) and (b) show a simulation result where TARGET is static on the coordinate: ${}^t(3.0, 1.5)$ and where each R_i rotates as: $\dot{\theta}_i(t) = 2.0\pi/2.5$ rad/s. We put two cylindrical obstacles. The center of one cylindrical obstacle is located on the coordinate: ${}^t(1.5, 4.0)$ and its radius is 0.5 m. The center of the other is located on the coordinate: ${}^t(4.5, 4.0)$ and its radius is also 0.5 m. We can see that the troop goes through the space between the obstacles and it achieves this cooperative behavior in this case.

Fig. 14(a) and (b) show a simulation result where TARGET is static on the coordinate: ${}^t(3.0, 2.0)$ and where each R_i rotates as: $\dot{\theta}_i(t) = 2.0\pi/2.5$ rad/s. We set the formation vectors of the eight robots as: ${}^t(d_{x1}, d_{y1}) = {}^t(-2.2, -1.6)$, ${}^t(d_{x2}, d_{y2}) = {}^t(-1.0, 0.8)$, ${}^t(d_{x3}, d_{y3}) = {}^t(-0.6, 1.6)$, ${}^t(d_{x4}, d_{y4}) = {}^t(-0.2, 4.0)$, ${}^t(d_{x5}, d_{y5}) = {}^t(0.2, 4.0)$, ${}^t(d_{x6}, d_{y6}) = {}^t(0.6, 1.6)$, ${}^t(d_{x7}, d_{y7}) = {}^t(1.0, 0.8)$, and ${}^t(d_{x8}, d_{y8}) = {}^t(2.2, -1.6)$. Since, as we have

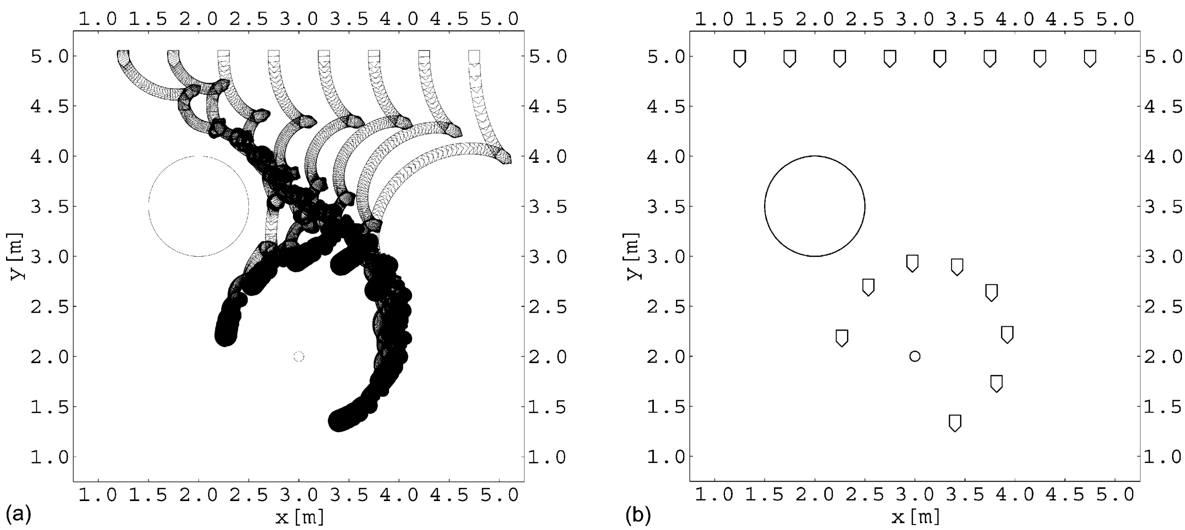

Fig. 12. Evolutions of robot positions and orientations. (a) $t = 0.0$–30.0 s; (b) $t = 0.0, 30.0$ s.

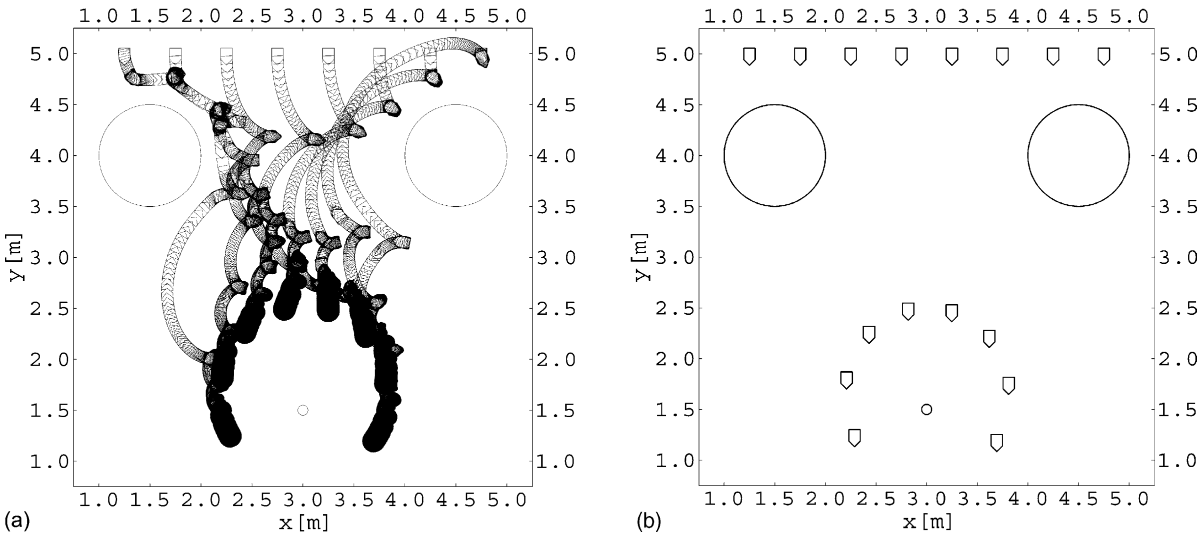

Fig. 13. Evolutions of robot positions and orientations. (a) $t = 0.0$–30.0 s; (b) $t = 0.0$, 30.0 s.

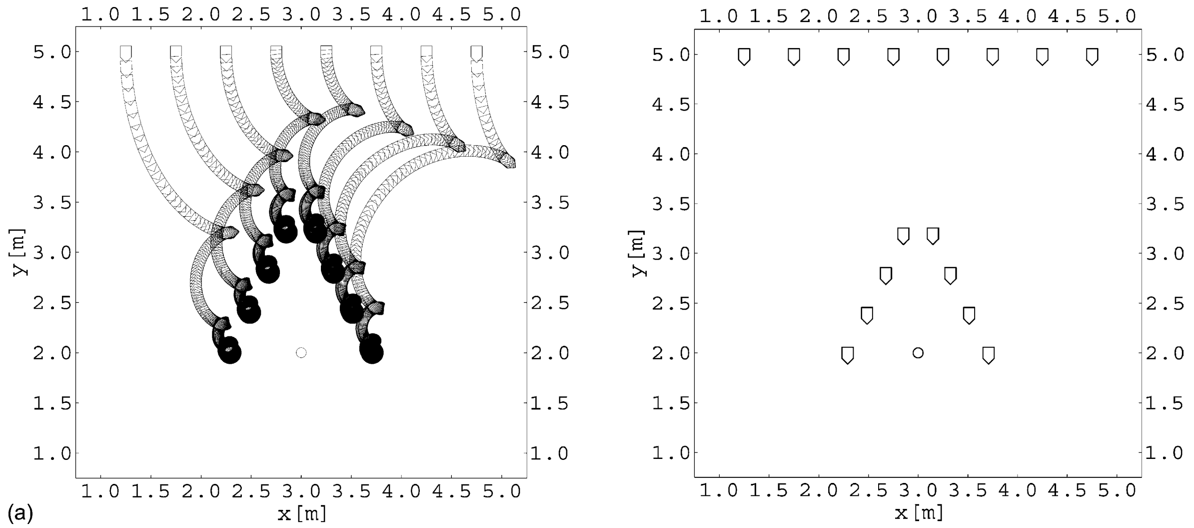

Fig. 14. Evolutions of robot positions and orientations. (a) $t = 0.0$–30.0 s; (b) $t = 0.0$, 30.0 s.

described, the formation is controllable by the formation vectors, it is possible to make the troop have other formations by controlling the vectors. We can see that the troop makes a triangle formation around TARGET in this case. These simulations are performed by the Runge–Kutta–Gill method and its sampling time is 0.005 s.

6. Conclusions

This paper has presented a distributed smooth time-varying feedback control law which asymptotically stabilizes multiple nonholonomic mobile robots of the Hilare-type to capture/enclose a target/invader by making troop formations in surveillance areas, and whose asymptotic stability is guaranteed in a mathematical framework, averaging theory. We have specifically dealt with a matrix whose components are averaged over time by integration and whose eigenvalue distribution explicitly describes stability of this control law. The eigenvalue distribution is analytically shown by Hölder's inequality in functional analysis, which means that stability analysis of this control law is given in averaging theory and it is technically related with functional analysis. Each robot in this control law has a two-dimensional control input referred to as a "formation vector" and the formation is controllable by the vectors. Especially, the final relative position of the troop to the target and its final formation around it are given as a convergence value of a first-order linear time-differential equation that is time-invariant while this control law is time-varying. As for determining the formation vectors, we have used a reactive control framework in which each robot has some reactions heuristically designed according to this cooperative hunting behavior. Therefore, this robotic system is a hybrid system that consists of a distributed smooth time-varying feedback control law and a reactive control framework. The validity of this hybrid system is supported by computer simulations.

References

[1] Y. Aiyama, M. Hara, T. Yabuki, J. Ota, T. Arai, Cooperative transportation by two four-legged robots with implicit communication, Robotics and Autonomous Systems 29 (1) (1999) 13–19.

[2] T. Arai, J. Ota, Dwarf intelligence—a large object carried by seven dwarves, Robotics and Autonomous Systems 18 (1996) 149–155.

[3] T. Balch, R.C. Arkin, Behavior-based formation control for multi-robot teams, IEEE Transactions on Robotics and Automation 14 (6) (1999) 926–939.

[4] T. Balch, M. Hybinette, Social potentials for scalable multi-robot formations, in: Proceedings of the 2000 IEEE International Conference on Robotics and Automation, San Francisco, CA, 2000, pp. 73–80.

[5] A.M. Bloch, M. Reyhanoglu, N.M. McClamroch, Control and stabilization of nonholonomic dynamic systems, IEEE Transactions on Automatic Control 37 (11) (1992) 1746–1757.

[6] J. Borenstein, Y. Koren, Real-time obstacle avoidance for fast mobile robots, IEEE Transactions on Robotics and Automation 19 (5) (1989) 1179–1187.

[7] R.W. Brockett, Asymptotic stability and feedback stabilization, in: R.W. Brockett, R.S. Millman, H.J. Sussman (Eds.), Differential Geometric Control Theory, Birkhauser, Boston, MA, 1983, pp. 181–208.

[8] R.A. Brooks, P. Maes, M.J. Mataric, G. More, Lunar base construction robots, in: Proceedings of the 1990 IEEE/RSJ International Workshop on Intelligent Robots and Systems (IROS'90), Tsuchiura, Tsukuba, Japan, 1990, pp. 389–392.

[9] W. Burgard, D. Fox, M. Moors, R. Simmons, S. Thrun, Collaborative multi-robot exploration, in: Proceedings of the 2000 IEEE International Conference on Robotics and Automation (ICRA'2000), San Francisco, CA, 2000, pp. 476–481.

[10] C. Canudas de Wit, O.J. Sørdalen, Exponential stabilization of mobile robots with nonholonomic constraints, IEEE Transactions on Automatic Control 37 (11) (1992) 1791–1797.

[11] J.-M. Coron, Global asymptotic stabilization for controllable systems without drift, Mathematics of Control, Signals and Systems 5 (3) (1992) 295–312.

[12] A. De Luca, G. Oriolo, C. Samson, Feedback control of a nonholonomic car-like robot, in: J.P. Laumond (Ed.), Robot Motion Planning and Control, Lectures Notes in Control and Information Sciences, Springer, Berlin, 1998, pp. 171–253.

[13] J. Desai, J.P. Ostrowski, V. Kumar, Controlling formations of multiple mobile robots, in: Proceedings of the 1998 IEEE International Conference on Robotics and Automation (ICRA'98), Leuven, Belgium, 1998, pp. 2864–2869.

[14] J. Desai, V. Kumar, J.P. Ostrowski, Control of changes in formation for a team of mobile robots, in: Proceedings of the 1999 IEEE International Conference on Robotics and Automation (ICRA'99), Detroit, MI, May 1999, pp. 1556–1561.

[15] B. Donald, L. Gariepy, D. Rus, Distributed manipulation of multiple objects using ropes, in: Proceedings of the 2000 IEEE International Conference on Robotics and Automation (ICRA'2000), San Francisco, CA, 2000, pp. 450–457.

[16] R. Fierro, A.K. Das, V. Kumar, J.P. Ostrowski, Hybrid control of formations of robots, in: Proceedings of the 2001 IEEE International Conference on Robotics and Automation (ICRA 2001), Seoul, Korea, May 2001, pp. 157–162.

[17] D.W. Gage, Command control for many-robot systems, Unmanned Systems 10 (4) (1992) 28–34.

[18] G. Giralt, R. Sobek, R. Chatila, A multi-level planning and navigation system for a mobile robot: a first approach to Hilare, in: Proceedings of the Sixth International Joint Conference on Artificial Intelligence, Tokyo, 1979, pp. 335–337.

[19] P.J. Johnson, J.S. Bay, Distributed control of simulated autonomous mobile robot collectives in payload transportation, Autonomous Robots 2 (1) (1995) 43–63.

[20] O. Khatib, Real-time obstacle avoidance for manipulators and mobile robots, International Journal of Robotics Research 5 (1) (1980) 90–98.

[21] O. Khatib, Y. Yokoi, K. Chang, D. Ruspini, R. Holmberg, A. Casal, Coordination and decentralized cooperation of multiple mobile manipulators, Journal of Robotic Systems 13 (11) (1996) 755–764.
[22] O. Khatib, Mobile manipulation: the robotic assistant, Robotics and Autonomous Systems 26 (2–3) (1999) 175–183.
[23] S. Kodama, N. Suda, Matrix Theory for System Controls, Society of Instrument and Control Engineers, 1978 (in Japanese).
[24] C.R. Kube, H. Zhang, Task modeling in collective robots, Autonomous Robots 4 (1) (1997) 53–72.
[25] C.R. Kube, E. Bonabeau, Cooperative transport by ants and robots, Robotics and Autonomous Systems 30 (2000) 85–101.
[26] J.C. Latombe, Robot Motion Planning, Kluwer Academic Publishers, Boston, MA, 1990.
[27] M.J. Mataric, M. Nilsson, K.T. Simsarin, Cooperative multi-robot box-pushing, in: Proceedings of the 1995 IEEE/RSJ International Conference on Intelligent Robots and Systems (IROS'95), Pittsburgh, PA, USA, 1995, pp. 556–561.
[28] R.T. M'Closkey, R.M. Murray, Exponential stabilization of driftless nonlinear control systems using homogeneous feedback, IEEE Transactions on Automatic Control 42 (5) (1997) 614–628.
[29] T. Orwig, Cybermotion's roving robots, Industrial Robot 20 (3) (1993) 27–29.
[30] L.E. Parker, ALLIANCE: an architecture for fault-tolerant multi-robot cooperation, IEEE Transactions on Robotics and Automation 14 (2) (1998) 220–240.
[31] J.-B. Pomet, Explicit design of time-varying stabilizing control laws for a class of controllable systems without drift, Systems and Control Letters 18 (2) (1992) 147–158.
[32] C. Samson, Velocity and torque feedback control of a nonholonomic cart, in: Proceedings of International Workshop on Nonlinear Adaptive Control: Issues in Robotics, Advanced Robot Control, Vol. 162, Springer, New York, 1991, pp. 125–151.
[33] C. Samson, Control of chained systems: application to path following and time-varying point-stabilization of mobile robots, IEEE Transactions on Automatic Control 40 (1) (1995) 64–77.
[34] J.A. Sanders, F. Verhulst, Averaging Methods in Nonlinear Dynamical Systems, Springer, New York, 1985.
[35] O.J. Sørdalen, O. Egeland, Exponential stabilization of nonholonomic chained systems, IEEE Transactions on Automatic Control 40 (1) (1995) 35–49.
[36] S.A. Stoeter, P.E. Rybski, M.D. Erickson, M. Gini, D.F. Hougen, D.G. Krantz, N. Papanikolopoulos, M. Wyman, A robot team for exploration and surveillance: design and architecture, in: Proceedings of the International Conference on Intelligent Autonomous Systems 6, Venice, Italy, July 2000, pp. 767–774.
[37] K. Sugihara, I. Suzuki, Distributed motion coordination of multiple mobile robots, in: Proceedings of the 1990 International Symposium on Intelligent Control, 1990, pp. 138–143.
[38] K. Sugihara, I. Suzuki, Distributed algorithms for formation of geometric patterns with many mobile robots, Journal of Robotic Systems 13 (3) (1996) 127–139.
[39] A.R. Teel, R.M. Murray, G. Walsh, Non-holonomic control systems: from steering to stabilization with sinusoids, International Journal of Control 62 (4) (1995) 849–870.
[40] H. Yamaguchi, Studies of distributed autonomous control for mobile robot groups, Doctoral Dissertation, The University of Tokyo, 1995.
[41] H. Yamaguchi, G. Beni, Distributed autonomous formation control of mobile robot groups by swarm-based pattern generation, in: Proceedings of the 1996 International Symposium of Distributed Autonomous Robotic Systems (DARS'98), Springer, Berlin, 1996, pp. 141–155.
[42] H. Yamaguchi, Adaptive formation control for distributed autonomous mobile robot groups, in: Proceedings of the 1997 IEEE International Conference on Robotics and Automation (ICRA'97), Albuquerque, NM, USA, 1997, pp. 2300–2305.
[43] H. Yamaguchi, A cooperative hunting behavior by mobile robot troops, in: Proceedings of the 1998 IEEE International Conference on Robotics and Automation (ICRA'98), Leuven, Belgium, 1998, pp. 3204–3209.
[44] H. Yamaguchi, J.W. Burdick, Asymptotic stabilization of multiple nonholonomic mobile robots forming group formations, in: Proceedings of the 1998 IEEE International Conference on Robotics and Automation (ICRA'98), Leuven, Belgium, 1998, pp. 3573–3580.
[45] H. Yamaguchi, A cooperative hunting behavior by multiple nonholonomic mobile robots, in: Proceedings of the 1998 IEEE International Conference on Systems, Man and Cybernetics (SMC'98), San Diego, CA, USA, 1998.
[46] H. Yamaguchi, J.W. Burdick, Time-varying feedback control for nonholonomic mobile robots forming group formations, in: Proceedings of the 1998 IEEE Conference on Decision and Control (CDC'98), Tampa, FL, USA, 1998, pp. 4156–4163.
[47] H. Yamaguchi, A cooperative hunting behavior by mobile robot troops, International Journal of Robotics Research 18 (8) (1999) 931–940.
[48] H. Yamaguchi, T. Arai, G. Beni, A distributed control scheme for multiple robotic vehicles to make group formations, Robotics and Autonomous Systems 36 (4) (2001) 125–147.
[49] H. Yamaguchi, T. Arai, A distributed navigation strategy for multiple mobile robots to make group formations adapting to geometrical constraints, JSME International Journal, Series C 45 (3) (2002) 758–766.
[50] A. Yamashita, M. Fukuchi, J. Ota, T. Arai, H. Asama, Motion planning for cooperative transportation of a large object by multiple mobile robots in a 3D environment, in: Proceedings of the 2000 IEEE International Conference on Robotics and Automation (ICRA'2000), San Francisco, CA, 2000, pp. 3144–3151.
[51] K. Yosida, Functional Analysis, 6th ed., Springer, Berlin, 1980.

Hiroaki Yamaguchi received the B.S., M.S. and Ph.D. degrees all from the University of Tokyo in 1990, 1992 and 1995, respectively. He did research in distributed robotics at the University of California, Riverside, as a Postdoctoral Fellow from 1995 to 1996, and in nonlinear control theory for distributed robotics as a Postdoctoral Scholar at California Institute of Technology (CalTech) from 1996 to 1998. He has spent two years as a Research Associate at Research into Artifcats, Center for Engineering (RACE), the University of Tokyo, on studying motion planning and control for highly nonlinear mechanical systems such as coupled vehicle combinations. He is currently an Assistant Professor at Department of Systems Information Engineering, Musashi Institute of Technology, Tokyo, Japan. His research interests are distributed robotics, nonlinear mechanics and control.